NASA CONTRACTOR
REPORT

NASA CR-144294

SPACE PROCESSING FLOAT ZONE THERMAL ANALYSIS

By J. T. Pogson and D. M. Anderson

The Boeing Company
Seattle, Washington

May 1976

(NASA-CR-144294) SPACE PROCESSING FLOAT ZONE THERMAL ANALYSIS (Boeing Co., Seattle, Wash.) 62 p HC $4.50 CSCL 20B

N76-25059

Unclas
G3/76 28245

Prepared for

NASA-GEORGE C. MARSHALL SPACE FLIGHT CENTER
Marshall Space Flight Center, Alabama 35812

RECEIVED
NASA STI FACILITY
INPUT BRANCH

TECHNICAL REPORT STANDARD TITLE PAGE

1. REPORT NO.	2. GOVERNMENT ACCESSION NO.	3. RECIPIENT'S CATALOG NO.
NASA CR-144294		

4. TITLE AND SUBTITLE	5. REPORT DATE
Space Processing Float Zone Thermal Analysis	May 1976
	6. PERFORMING ORGANIZATION CODE

7. AUTHOR(S)	8. PERFORMING ORGANIZATION REPORT #
J. T. Pogson and D. M. Anderson	

9. PERFORMING ORGANIZATION NAME AND ADDRESS	10. WORK UNIT NO.
The Boeing Company Seattle, Washington	11. CONTRACT OR GRANT NO. NAS8-31635

12. SPONSORING AGENCY NAME AND ADDRESS	13. TYPE OF REPORT & PERIOD COVERED
National Aeronautics and Space Administration Washington, D. C. 20546	Contractor
	14. SPONSORING AGENCY CODE

15. SUPPLEMENTARY NOTES

Prepared under the technical monitorship of James M. Zwiener, Space Sciences Laboratory, Marshall Space Flight Center, Alabama 35812

16. ABSTRACT

Two thermal analysis (BETA) computer program adaptations were prepared to analyze phase change histories in crystal specimens: the first program (BETA-CYL) treats right circular cylinder configurations and the second, more general, program (BETA-BOR) treats a generalized body-of-revolution configuration. A series of computer runs were made for silicon material to determine boundary conditions which produce flat solidification interfaces while, at the same time, minimizing peak temperatures in the molten zone. Flat solidification interfaces are a goal believed by some investigators to be required to produce high quality semiconductor materials. The thermal effects of convection in a molten zone were examined and found to be negligible in comparison to the conduction heat transfer of the melt.

17. KEY WORDS	18. DISTRIBUTION STATEMENT
	Unclassified — Unlimited

Charles A. Lundquist

Charles A. Lundquist
Director, Space Sciences Laboratory

19. SECURITY CLASSIF. (of this report)	20. SECURITY CLASSIF. (of this page)	21. NO. OF PAGES	22. PRICE
Unclassified	Unclassified	58	NTIS

TABLE OF CONTENTS

	PAGE
LIST OF FIGURES	iv
LIST OF TABLES	v
1.0 INTRODUCTION	1
2.0 ANALYSIS	2
3.0 DISCUSSION OF RESULTS	4
3.1 Cylindrical Melt Zones	5
3.2 Body of Revolution Melt Zones	9
CONCLUSIONS	11

ORIGINAL PAGE IS
OF POOR QUALITY

LIST OF FIGURES

		PAGE
FIGURE 1	MATH MODEL	15
2	BETA PROGRAM - CRYSTAL MELT/FREEZE TRANSIENT STUDY	16
3	HEAT PULSE SUBROUTINE (QSFC)	17
4	RUN 49 & 55 - LOCAL SURFACE HEAT FLUX PROFILES	18
5	PHASE CHANGE SUBROUTINE (PHAS)	19
6	RUN 71 - TEMPERATURE GRADIENT & HEAT FLUX PROFILES	20
7	RUN 71 - MELT ZONES	21
8	RUN 75 STEADY-STATE - NO CONVECTION	23
9	RUN 82 STEADY STATE - INFINITE CONVECTION	24
10	RUN 29 MELT ZONES	25
11	RUN 36 MELT ZONES	27
12	RUN 39 MELT ZONES	29
13	RUN 40 MELT ZONES	30
14	RUN 44 MELT ZONES	32
15	RUN 49 MELT ZONES	34
16	RUN 55 MELT ZONES	37
17	RUN 56 MELT ZONES	38
18	RUN 60 MELT ZONES	41
19	RUN 62 MELT ZONES	43
20	RUN 65 MELT ZONES	45
21	SURFACE HEAT FLUX RUN 56 & 60	47
22	SURFACE HEAT FLUX RUN 62	48
23	RUN 60 - TEMPERATURE GRADIENT & HEAT FLUX PROFILES	49
24	RUN 62 - TEMPERATURE GRADIENT & HEAT FLLX PROFILES	50
25	RUN 65 - TEMPERATURE GRADIENT & HEAT FLUX PROFILES	51
26	TYPICAL BODY OF REVOLUTION CONFIGURATIONS	52
27	BODY OF REVOLUTION NODE MAP	53
28	RUN 80 - MELT ZONE - TIME = 0	54
29	RUN 80 - MELT ZONE - TIME = 2.852 MIN.	55
30	RUN 72 - MELT ZONE NODE MAP	56
31	MELT ZONE TIME = 0 RUN 72	57
32	MELT ZONE TIME = 7.8 MIN. RUN 72	58

LIST OF TABLES

		Page
TABLE 1	COMPUTER RUN SUMMARY	12
2	SILICON THERMAL CONDUCTIVITY	13
3	SILICON SPECIFIC HEAT	14

1.0 INTRODUCTION

Growth of single crystals in vertical arc-imaging furnaces has been successfully demonstrated by various researchers. Early experiments with these furnaces using a carbon-arc energy source, encountered difficulties in maintaining uniform light intensity for required periods of time. Development of high-power Xenon arc lamps substantially reduced the instability problem experienced with carbon-arcs, and also allowed longer-term operation for crystal growth. Experiments have shown that one of the preferred approaches for growing single crystals in arc-imaging furnaces is the pedestal technique. This technique has alternatively been labeled a modified Czochralski, or modified float-zone process. The principal advantage of the float-zone process over other crystal growth techniques is production of higher purity crystals; achieved by eliminating the need for a crucible and the resulting crucible contamination. The homogeneity of crystals grown by the float-zone process, as with other processes, is affected by circulation patterns in the molten semi-conductor material. Carruthers and Grasso have extensively studied the stability and fluid flow in floating zones in both a simulated zero-gravity environment and on Skylab. Effects of convection patterns on homogeneity of solute distribution and electrical resistivity have been reviewed by Benson. Similar considerations should apply to float-zone crystal growth, and indicate that for the Czochralski process, all convection in the melt should be avoided.

Growth of single crystals in space is expected to substantially improve the solute homogeneity of crystals, by reducing or eliminating convection within the melt region. It should also be possible to form larger diameter crystals because the length of the suspended liquid zone can be increased in the absence of gravity.

Maintaining a large-diameter uniform-temperature melt zone will be a key problem in designing a crystal growth experiment using a solar concentrator. Accordingly, this study has been directed at thermal modeling of the liquid zone to predict temperature gradients for various parametric changes.

2.0 ANALYSIS

Two generalized lumped parameter nodal math models were formulated to represent a right circular cylindrical, BETA-CYL, and a body of revolution configuration, BETA-BOR, with time varying boundary conditions. The physical system was sectioned into an array of discrete volumes and the mass of each volume element was "lumped" at a point within the volume which it represented. The paths for heat transfer from one mode to another were represented by conductors joining the appropriate nodes. The thermal models each contained a maximum of 300 nodes, Figure (1) depicts the right circular cylindrical nodal math model.

The thermal math models described above were input into the Boeing Engineering Thermal Analyzer Program (BETA). This program solves an electrical analog network system using an iterative numerical method. Both transient and steady state solutions are treated. A logic diagram of the computer program detailing the computational steps is given in Figure (2). Several BETA subroutines required development to permit numerical simulation of the applied heat flux boundary conditions and the change of phase process.

The heat pulse subroutine is illustrated in Figure (3). This permits the specification of an externally applied heat flux of the form:

$$q_i = q_o \, e^{-A|X-Vt-B|^2}$$

where:

- q_o - Peak surface heat flux, Btu/min-in^2
- X - Distance from reference end of crystal, inches
- V - Pulse velocity away from reference end of crystal, in/min
- t - Time elapsed since start of pulse movement, min
- B - Starting position of center of pulse measured from reference end of crystal, inches
- A - Pulse width parameter

Values of A of 100 and 4 were used, the relative widths of the heat pulses can be seen in Figure 4.

A similar cooling subroutine was also formulated to represent surface cooling.

During a phase change each node must receive or release a quantity of energy equal to its latent heat of fusion. This energy exchange accounting system was simulated by a phase change subroutine, PHAS. Figure (5) illustrates the logic system. Each node is surveyed to see if it is at or undergoing a phase change. If it is undergoing a phase change then an accounting system keeps the nodal temperature constant at the melting temperature until the energy exchange matches the node latent heat of fusion.

This study did not directly consider the transparency of silicon to thermal radiation; however, the "no convection" and "Infinite convection" extremes considered for energy transport in the molten zone could be expected to bound the effects which might be observed had internal radiation been considered. Furthermore, with a cylindrical crystal, any radiation interchange between the surroundings and crystal internal regions due to transparency can only tend to reduce radial temperature gradients and consequently give a more uniform axial flow of thermal energy which is required to obtain flat interfaces. Radiation interchange in the axial direction, between internal crystal regions, was not expected to be very significant as temperature differences within the crystal are much less than temperature differences which exist between the crystal and its surroundings.

3.0 DISCUSSION OF RESULTS

A total of 82 runs were made to de-bug, checkout, and perform production analyses for this study. Only the runs shown in Table 1 contained significant results. The other runs, although more numerous, were less significant in terms of expended machine time.

The first block on this table describes the crystal configuration for each run and refers to a right circular cylinder unless otherwise stated. The right circular cylinder crystals were considered to consist of 30 wafers of equal thickness as defined by planes normal to the cylinder axis (see "Wafer Thickness" column).

The surface heat flux refers to the peak surface heat flux of a Gaussian shaped pulse when the word "Gauss" appears in the "Pulse Width" column. If the word "Uniform" appears in the "Pulse Width" column, the surface heat flux value applies over the entire heated length, and the number appearing in the "Pulse Width" column is the heated length, in inches, of a section of cylinder centered along the cylinder axis.

For some runs, the peak surface heat flux, q_0, was reduced linearly with time; the q_0 limits where applicable, are described in the "Surface Heat Flux" column. In any case, when the run time, i.e. "Real Time" in the "Time Data" block, exceeds the time shown in the "Heat Time" column, the heat is reduced to zero after the "Heat Time" shown.

In the "Number of Nodes" column, "300" indicates that each wafer was considered to consist of 10 rings, the temperatures of which were computed as node temperatures by the program. The number "120" indicates each wafer was considered to consist of 4 rings.

Under the "Cooling Parameters" block, the "Sink Temperature" and "Script F" define radiation rates from the radial surface of the crystal for the axial length of surface specified in the "Cooled Area" column. The ends; normal to the cylinder axis, were considered insulated for all runs.

Except for Runs 35, 72, 75, 80, 81, and 82, the initial temperature, uniform throughout the crystal, was one degree Fahrenheit below the melting point. This was done to prevent wasted computer time raising the crystal to the melting point. Runs 72, 75, 80, 81, and 82 were intended to determine steady state conditions and estimates of the final temperatures were used as initial temperatures for the analysis to conserve machine time, i.e., initial temperatures above the melting point were used in the heated region, and temperatures somewhat below the melting point were used in the cooled region.

Run 35 was a check of the program against an analytical solution for a cylinder, with uniform constant surface heat flux, using an initial uniform temperature of zero; excellent agreement was obtained.

3.1 Cylindrical Melt Zones

The initial part of this study consisted of analyzing cylindrical specimens (BETA-CYL program) on a transient basis using a constant strength heat source moving in the axial direction with ends cooled by radiation to a 70°F environment as shown below:

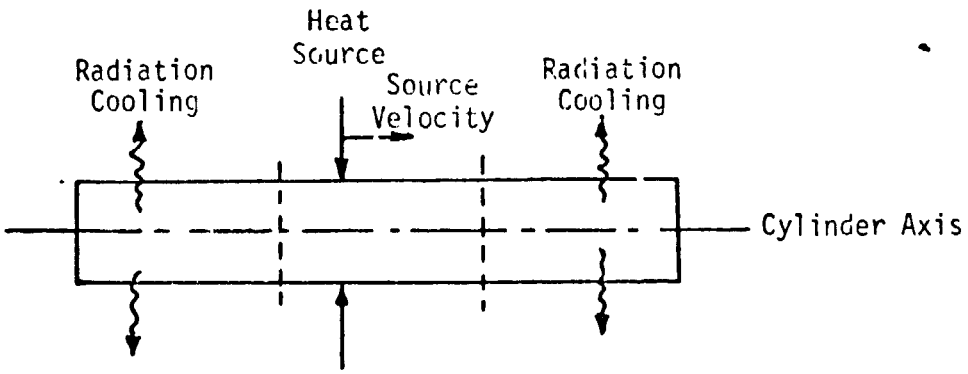

The source of the incident radiant energy was not modeled since it was considered that it could be best treated after determining the boundary conditions required to produce flat interfaces. The following parameters were varied in the transient analyses: heated length, cooled length, specimen diameter, constant source strength (moving heat sources), and transient source strength (moving and fixed heat sources). It was determined that an adiabatic section

between the heated and cooled sections would be beneficial in producing flat interfaces. Additionally, it was found that excessive machine time was required with a transient-type analysis due to the rather low solidification rate required for growth of high-perfection crystals ($\approx$1 cm/hr). A preferable analytical technique, in comparison to the transient analysis, for treating the continuous zone refinement/growth along a rod was to obtain the steady-stage solutions for configurations with stationary boundary conditions which give flat interfaces. If an extremely slow feed rate of the specimen is then introduced after steady state is achieved, a negligible change in the shape and location of the interfaces would occur with respect to a fixed reference system. Machine time required to solve for steady-state conditions is nominal provided that reasonable estimates of the final conditions are provided as inputs.

Figure 6 describes the conditions and results for Run 71. Excellent flat-interface solidification conditions were obtained and are shown in Figure 7. The physical state of each ring of each wafer has been represented in the computer printout by an "0", "1", or "2". Each column of figures represents a wafer of the crystal as defined in Table 1. The radial width of each wafer, as defined in the program, varies so that the volumes of each ring are equal regardless of the nominal ring radii. The figures are, therefore, not to scale in the radial direction. Since all wafers are the same thickness in the axial direction (for the right circular cylinder configuration) the printouts are to scale in the axial direction. The axis of the cylinder is indicated by a centerline at each end of the crystal. A "0" indicates that the state of that node is solid. A "1" indicates a molten state, and "2" indicates a partially melted state at the melting temperature. A column of zeros adjacent to a column of twos or ones indicates a flat solidification interface within a one-wafer-thickness tolerance. These printouts were used as a visual tool to allow rapid scanning of run results for each case. More exact definition of interface shapes can be determined by inspection of node freezing fraction data in the computer result numerical output.

The data printed at the left of each state are:

Time - minutes from start of analysis

$G_{A_{MAX}}$ - maximum axial temperature gradient, °F/inch

$G_{R_{MAX}}$ - maximum radial temperature gradient, °F/inch

T_{MAX} - maximum temperature, °F

A melting point temperature of 2573°F was assumed for silicon. Conductivity and specific heat values employed as a function of temperatures are shown in supplementary Tables 2 and 3.

Run 71 was for a 1-inch diameter crystal, 7.5 inches long with a stationary uniformly irradiating heat source applied to the central 2 inches of specimen. The source strength decayed linearly from 20 Btu/min-in^2 to 0 in the first 2 minutes of run time. For approximately 7 minutes after the heat source was shut off, the central molten zone solidified with virtually flat interfaces. The solidification rate was approximately 40 cm/hr, which is higher than current state of the art. The solidification process, however, could be increased to any desired duration by reducing the cooling rate at the crystal ends,e.g., through the use of louvers or radiation shields. The simulated high solidification rate was used here to conserve machine time. A lower cooling rate would be accompanied by lower temperature gradients in the crystal compared to those shown on Figures 6 and 7.

Figures 8 and 9 contain the computation for runs 75 and 82 respectively. A section through one half of the length of crystal is shown with each node defined by a rectangle (to scale), with resulting steady state temperatures given at each node in degrees F. The melt interface shape was sketched in based on freezing fraction data from the numerical output of the program.

A nearly converged solution using the steady state analysis technique was obtained with the case analyzed in Run 75; the corresponding conditions and results are shown on Figure 8. Although there was a slight deviation from flatness at the interface, it is believed that this could be eliminated by a slight reduction in the rate of

ORIGINAL PAGE IS OF POOR QUALITY

source irradiation which would move the interface into the insulated (shielded) region where the thermal flux lines are more nearly straight.

To bound the effects of convection in the molten zone, an "infinite convection" analysis was performed for the same configuration as in Run 75. This condition was implemented by assigning a cup-mixing temperature to the melt at each iteration which has the effect of instantaneously distributing throughout the melt zone all incident energy at the surface. The results are shown in Run 82, Figure 9. A virtually flat interface was obtained in almost the same position as with no convection. By comparing figures 8 and 9 it is seen that there is little difference in the two solutions except that the melt temperature with convection is uniform at a value somewhat lower than the peak value observed with no convection. The degree of convergency to a steady state solution can be assessed by noting how closely the total cooling rate approaches the constant heating rate. For Runs 75 and 82 the errors are 3% and 1% respectively, which is sufficient convergence for preliminary purposes.

Additional transient results, Runs 29, 36, 39, 40, 44, 49, 55, 56, 60, 62 and 65, similar to those presented for Run 71 are shown in Figures 10 through 20. The significant results for each of these runs are shown in the "Comments" column of Table 1.

Crystal specimen dimensions and boundary conditions are shown on Figures 4, 21, and 22 for Runs 49, 55, 56, 60, and 62. Of particular interest are the heat pulse shapes and positions on the specimen as a function of time which cannot be readily visualized from Table 1 data.

For Runs 60, 62, and 65 maximum axial and radial temperature gradients, maximum temperature, and peak surface heat flux are shown as a function of time on Figures 23, 24, and 25 respectively. The irregularities in the temperature and gradient curves are due to (1) the results of a lumped parameter thermal analysis, e.g. at the instant when a node melts or solidifies, a relatively sudden adjustment in adjacent node temperatures occurs, and (2) the location of the peak temperature and gradients moves around

in the crystal, whereas, the plots show only the peak values regardless of location in the crystal.

3.2 Body of Revolution Melt Zones

The body-of-revolution program (BETA-BOR) has the capability to analyze configurations where the specimen has a shape more complex than a right circular cylinder. Possible configurations of interest are shown on Figure 26: (a) vertical cylinder float zone with gravity (b) float-zone in Zero-G with rotation, and (c) crystal growth from different sized feed stock. An example of case (c) was analyzed for 6-inch and 12-inch rods meeting in a molten zone with an assumed curved section transition; the configuration and boundary conditions are shown on Figure 27. Estimates of steady state conditions used for program input are shown in Figure 28. Conditions after 2.85 minutes are shown on Figure 29. Steady state convergence is approached with a good flat solidification interface on the 12-inch end. The interface shapes were sketched in on Figure 29, based on melt fraction data from the program output for the respective interface nodes.

Figure 27 shows the locations of the nodes for Run 80 as limited by the ability of the node size to be resolved into cells on the printout page. The dashes and asterisks are used in an alternate fashion for each wafer to define the node boundaries for each wafer. Each wafer has 10 ring shaped nodes, however on the 6" diameter end, not all are shown due to the resolution limitation described above. The radial interfaces between the nodes in regions of body diameter change are considered by the program to be conical surfaces. The uniform irradiation rate shown for the heated area is based on actual surface area, not a correct area based on some assumed ray direction. The shape shown on the printout is approximately to scale.

Figure 28 shows the initial conditions for Run 80: an asterisk indicates a temperature above the melting point, a dash indicates a temperature below the melting point. The difference between this figure as compared to Figure 7 is that the symbols at each node correspond to the node state rather than alternating to define node boundaries. Final conditions are shown for Run 80 on Figure 29

ORIGINAL PAGE IS
OF POOR QUALITY

after the indicated elapsed time, given the Figure 28 initial conditions. Dashes and asterisks are as described for Figure 28 and an "X" symbol denotes a node partially melted at the melting temperature. Melt interface shapes shown are based on freezing fraction data for the melting nodes. Temperatures at selected points were shown for reference. Heating and cooling rates were shown as a guide to the deviation from steady state, i.e. if a true steady state had been reached, heating and cooling rates would be equal. This condition could be achieved by allowing the run to proceed in time, at a corresponding cost in machine time.

Figures 30, 31, and 32 show data similar to that of Figures 27, 28, and 29 which apply to Run 72; neither steady state conditions nor flat interfaces were obtained.

CONCLUSIONS

Thermal math models of a silicon float zone crystal growth process were formulated. Transient temperatures and melt zones were determined for a variety of simulated external heat flux conditions. It was found that nearly flat interface solidification conditions could be simulated by varying the applied heat flux, as in cases 65 and 71. Additionally, convective affects were found to be negligible in reducing temperature gradients.

Table 1. Computer Run Summary

Run	Cylinder configuration			Heating parameters					Nodes	Cooling parameters			Time data		Comments
	Diameter	Length	Water thickness	Surface heat peak flux	Pulse velocity	Heat time	Start pulse	Pulse width	Number of nodes	Sink temp	Script F	Cooled area	Real time	Mach time	
	(in.)	(in.)	(in.)	(Btu/min-in.^{2})	in./min	min	in. from end	▷1		°F			(min)	(cru)	
29	3	3	0.1	10,000	0.1	051	0.3	100 gauss	300	–	–	–	.051 trans	12.3	Initial run, stability check with extremely high heat flux. Peak surface temp 84,753° above melting point at end of run
39	3	3	0.1	10,000	0.1	051	0.3	100 gauss	300	–	–	–	.051 trans	9.9	Same as run 1, except added infinite convection and different phase map symbols, convection increases quantity of melting
35	3	3	0.1	Uniform surface heat flux–106 Btu/min-in.^{2}					300	–	–	–	1.0 trans	21.1	Check case for comparison with classical solution–cylinder with uniform surface heat flux–went thru PHAS subroutine with near zero heat of fusion to check subroutine. Excellent agreement with Carslaw Jaeger solution
36	3	9	0.3	600	0.3	6.	3.	4 gauss	300	70.	0.3	3" on each end	6.0 trans	52.0	Inadequate cooling–crystal melts out to ends–no convection. Peak surface temp = 4°,630°F above melting point
40	3	9	0.3	100	1.	3.	3	100 gauss	300	70.	0.3	3" on each end	3.4 trans	40.9	Inadequate heating–crystal didn't melt to center–no convection Peak surface temp = 331°F above melting point
41	0.7	6	0.2	200	1.4	1.0	2.3	100 gauss	300	70.	0.5	2" on each end	0.3 trans	66.1	Excessive machine time did not run to end of heating cycle. Peak surface temp = 1,757°F above melting point
44	1.5	6	0.2	238	1.4	1.0	2.3	100 gauss	120	70.	0.8	2" on each end	3.0 trans	17.2	Nearly uniform melt at end of minute 1,530° peak surface temp above melting point Flat interface at upstream end @ t = 2.51 min, flat interface at downstream end @ t = 2.73 min, flatness lost @ 2.95 min but may be small deviation
49	1.5	6	0.2	198 @ t=0 linear to 0 @ t = 3	.48	3.0	2.3	100 gauss	120	70.	0.8	2" on each end	10. trans	44.3	Flat upstream interface @ t = 1.83 min, lost briefly @ 2.6, flat on right end @ 4.04 Flatness lost on right end at 4.56, good to 5.35 min, two wafers selected under nearly flat conditions – 0.4" of good crystal Peak temp = 1,211°F above melt
55	1.5	6	0.2	7.9 @ t=0 linear to 0 @ t = 3	0	3.0	3.0	4 gauss	120	70.	0.8	2" on each end	6. trans	30.8	Only melted surface node and temp did not exceed melting point
56	1.5	6	0.2	40 @ t=0 linear to 0 @ t = 3	0	3.0	3.0	4 gauss	120	70.	0.8	2" on each end	6. trans	31.0	Symmetrical boundary conditions, stationary decaying heat pulse Flat interfaces from t = 3.47 to t = 5.37, 0.8" of good crystal in 1.9 minutes Peak temp = 607°F above melt
50	1.5	6	0.2	22.6 @ t=0 linear to 0 @ t = 4	0	4.0	3.0	4 gauss	120	70.	0.8	2" on each end	8 trans	35.9	Peak temp down to 379°F above melt. 0.4" good crystal, t = 4.4 to 4.9 min
62	1.0	7.5	0.25	18 @ t=0 linear to 0 @ t = 2	0	2.0	3.75	4 gauss	120	70	.5	2.5" on each end	5 trans	34.2	Not quite enough heat max surf temp = 125° above melt. No good crystal, interface never flattened
65	1.0	7.5	0.25	30 @ t=0 linear to 0 @ t = 2	0	2.0	3.75	2" uniform	120	70.	.5	2.5" on each end	5 trans	34.1	About 2" of good crystal but 1.2" left to solidify at 5 min
71	1.0	7.5	0.25	22 @ t=0 linear to 0 @ t = 2	0	2.0	-	2" uniform	120	70.	.5	2.0" on each end	10 trans	65.3	2" good crystal @ 40 cm/hr solification rate
75	1.0	7.5	0.25	3.5	0	∞	–	2" uniform	120	70.	.5	2.0" on each end	5 trans	37.3	Final temps guessed to start, near flat final interface and steady state obtained. Could infer infinite good crystal be feeding whole cylinder at very low rate (0.1 cm/hr)
81	1.0	7.5	0.25	3.5	0	∞	–	2" uniform	120	70.	.5	2.0" on each end	5 trans	33.7	Final temps guessed to start, same as run 75 except subroutines called every 64 iterations Didn't save much time and significantly different results occurred.
82	1.0	7.5	0.25	3.5	0	∞	–	2" uniform	120	70.	.5	2.0" on each end	5 trans	34.7	Sames conditions as run 75 except infinite convection added Near steady state achieved with flatter interface, but nearly the same as without convection except in melt region temperatures are uniform
72	BOR 6" to 12" dia 7.5 inches long			7.5 Btu/min-in.^{2} uniform over central 2.5" length					300	70.	.5	2."/2.5" each end	7.8 trans	43.3	Poor convergence to steady state. Interfaces not flat
80	BOR 6" to 12" dia 7.5 inches long			4.2 Btu/min-in.^{2} uniform over central 2.5" length					300	70	5	2"/2.5" each end	2.5 trans	40.4	Near convergence to steady state. Good interfaces

Initial condition is melting point minus one degree except runs 35, 75, 81, 82, 72, and 80

▷1 See Table 1 discussion in text for pulse width definition

ORIGINAL PAGE IS OF POOR QUALITY

SILICON THERMAL CONDUCTIVITY

TABLE 2

TEMP - °F	Thermal Conductivity Btu/min-in-°F
32	.1348
80.3	.1187
170.3	.0955
260.3	.0793
440.3	.0611
620.3	.0497
800.3	.0408
980.3	.0339
1160	.0287
1340	.0250
1520	.0223
1880	.0196
2440	.0178
2573	.0176
10^6	.0176

SILICON SPECIFIC HEAT

TABLE 3

TEMP - °F	Specific Heat - Btu/LB-°F
0	.157
200	.184
400	.197
600	.203
800	.208
1000	.211
1200	.216
1400	.220
1600	.224
1800	.228
2000	.234
2200	.242
2400	.245
2573	.249
2600	.250
10^6	.250

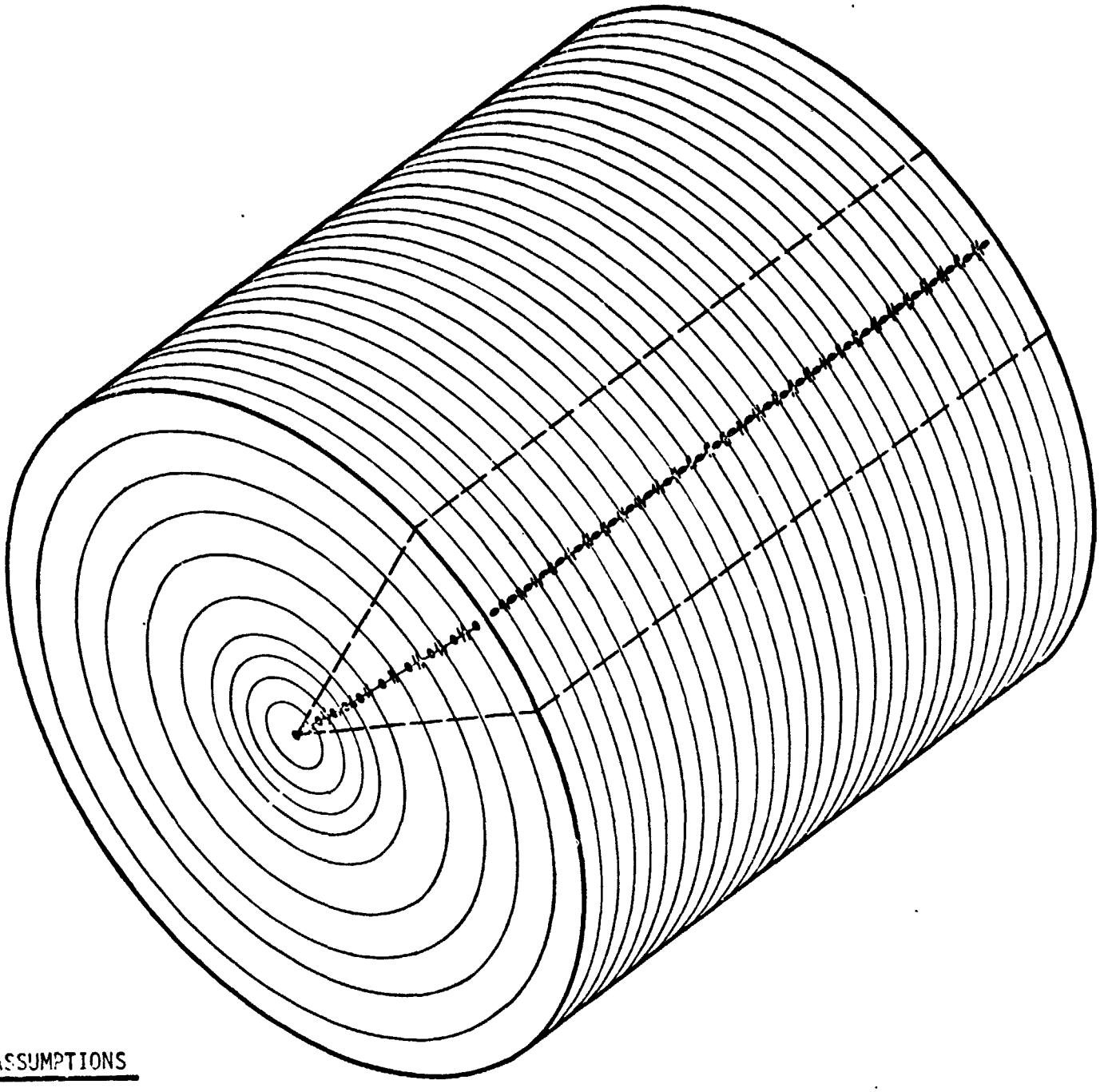

ASSUMPTIONS

- CENTER CORE + 9 RINGS FOR EACH WAFER - 30 WAFERS
- MASS OF EACH RING OF EACH WAFER IS LUMPED TO FORM NODE (300 NODES)
- ENDS ARE INSULATED
- MOVING GAUSSIAN SURFACE HEAT FLUX DISTRIBUTION

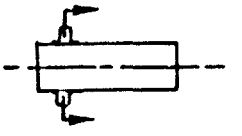

- SURFACE COOLING TO SURROUNDINGS BY RADIATION

FIGURE: 1 MATH MODEL

BETA PROGRAM - CRYSTAL MELT/FREEZE TRANSIENT STUDY

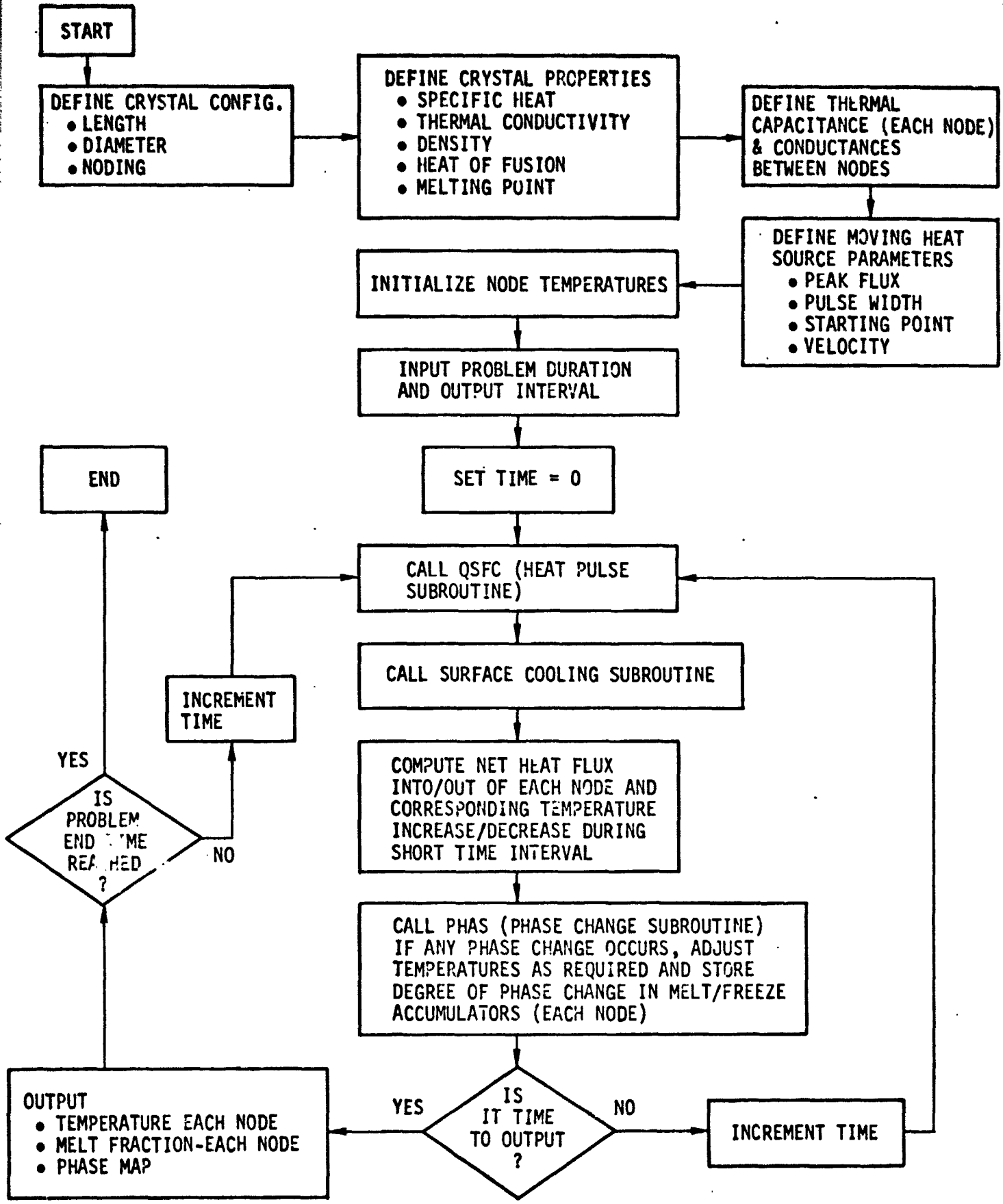

FIGURE: 2

ORIGINAL PAGE IS OF POOR QUALITY

HEAT PULSE SUBROUTINE (QSFC)

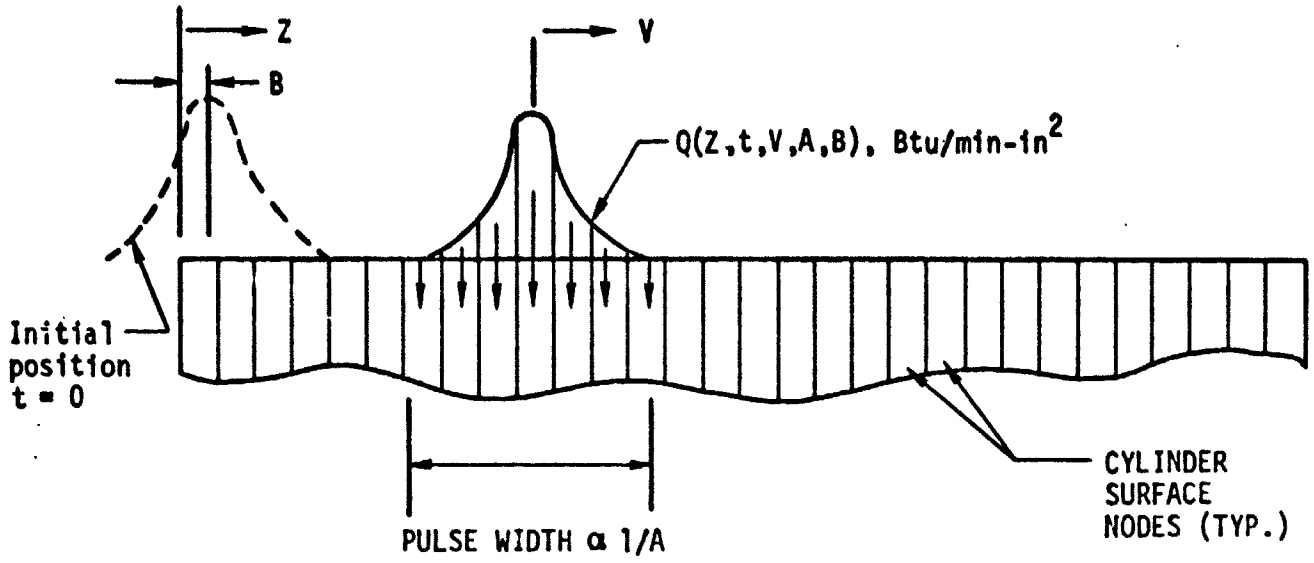

FLOW DIAGRAM

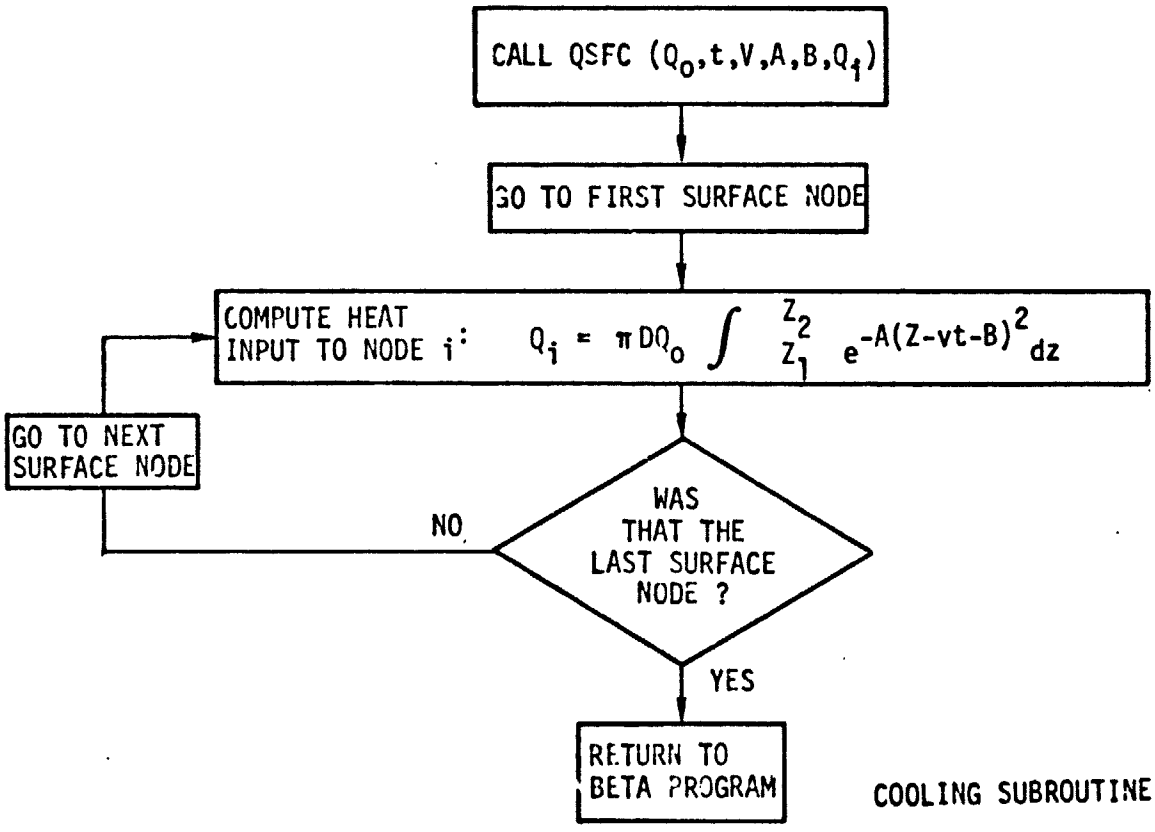

COOLING SUBROUTINE IS SIMILIAR

FIGURE: 3

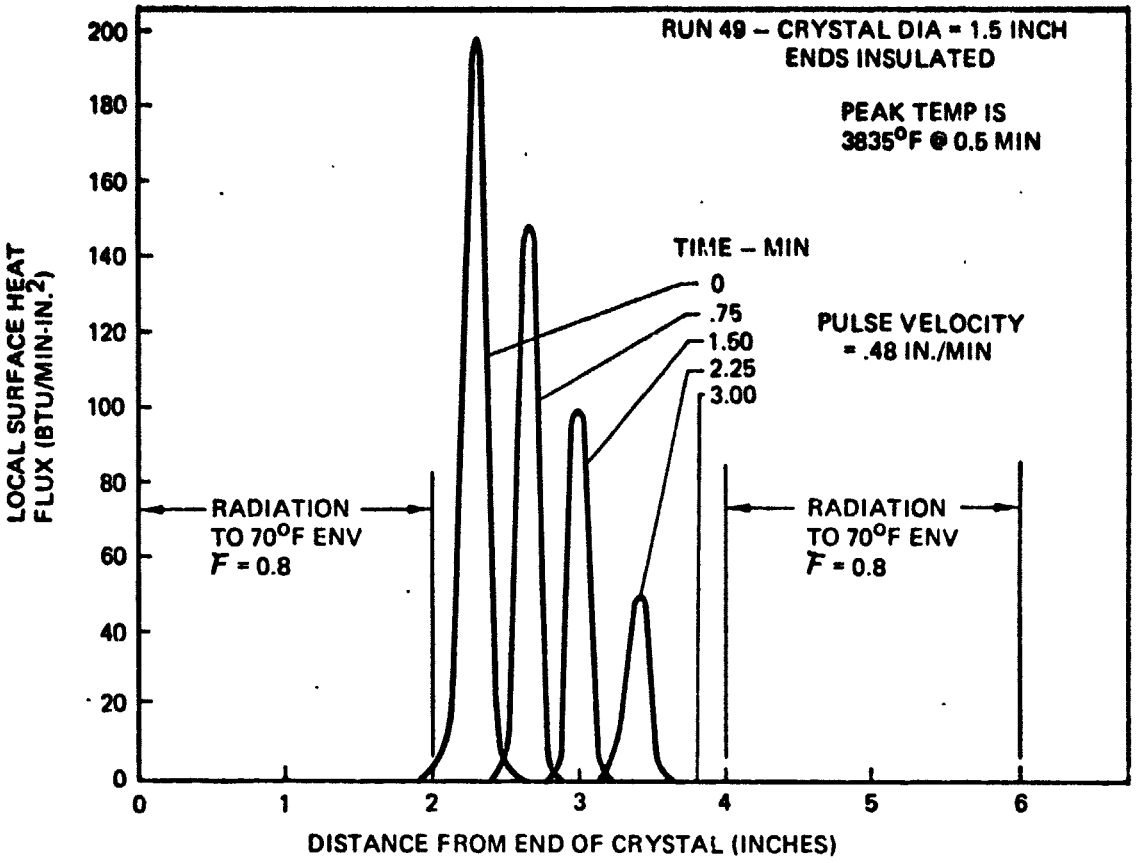

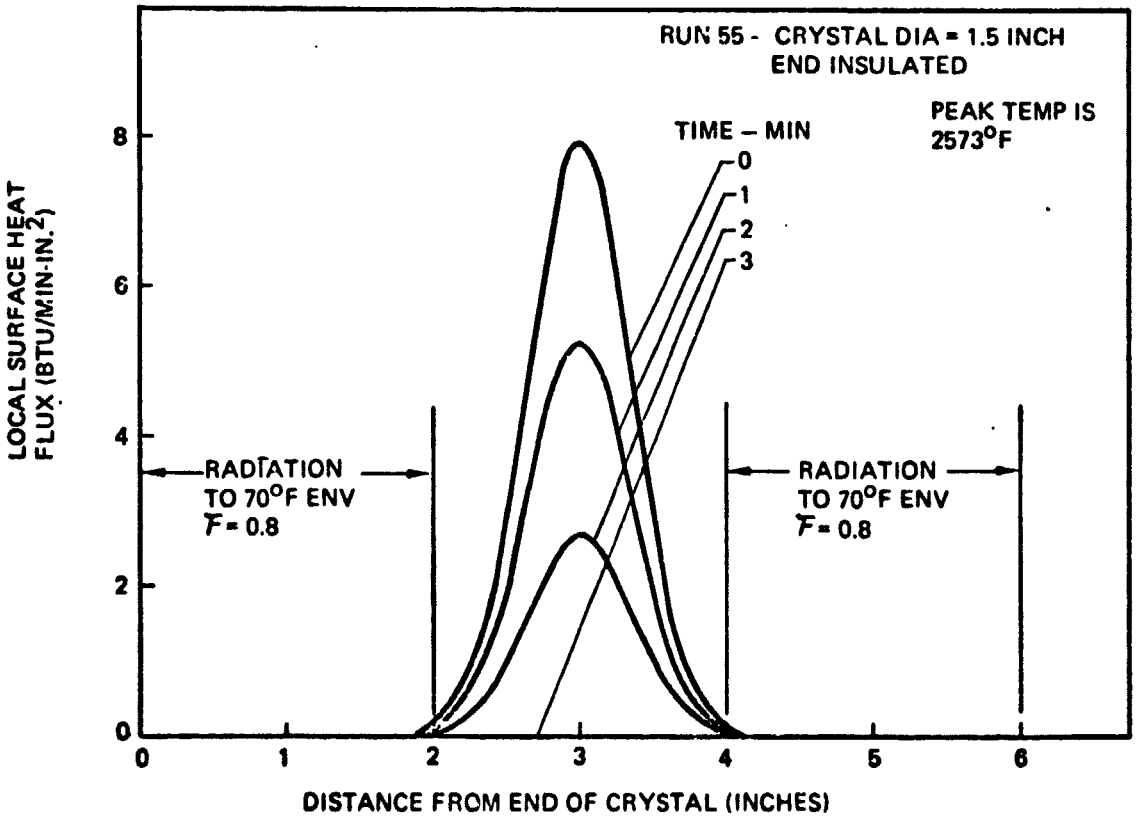

Figure 4

RUN 49 & 55 - LOCAL SURFACE HEAT FLUX PROFILES

PHASE CHANGE SUBROUTINE (PHAS)

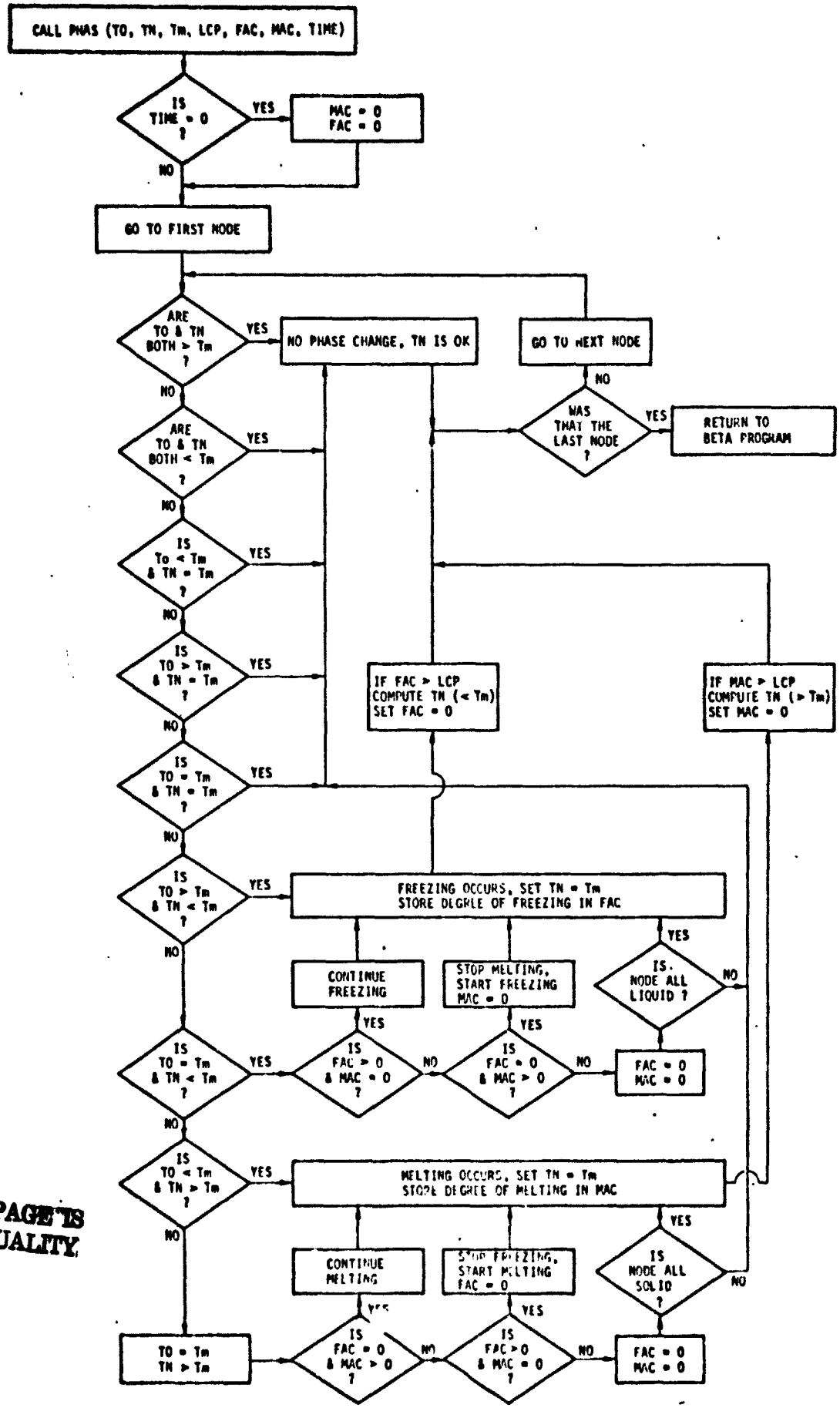

ORIGINAL PAGE IS
OF POOR QUALITY

FIGURE: 5

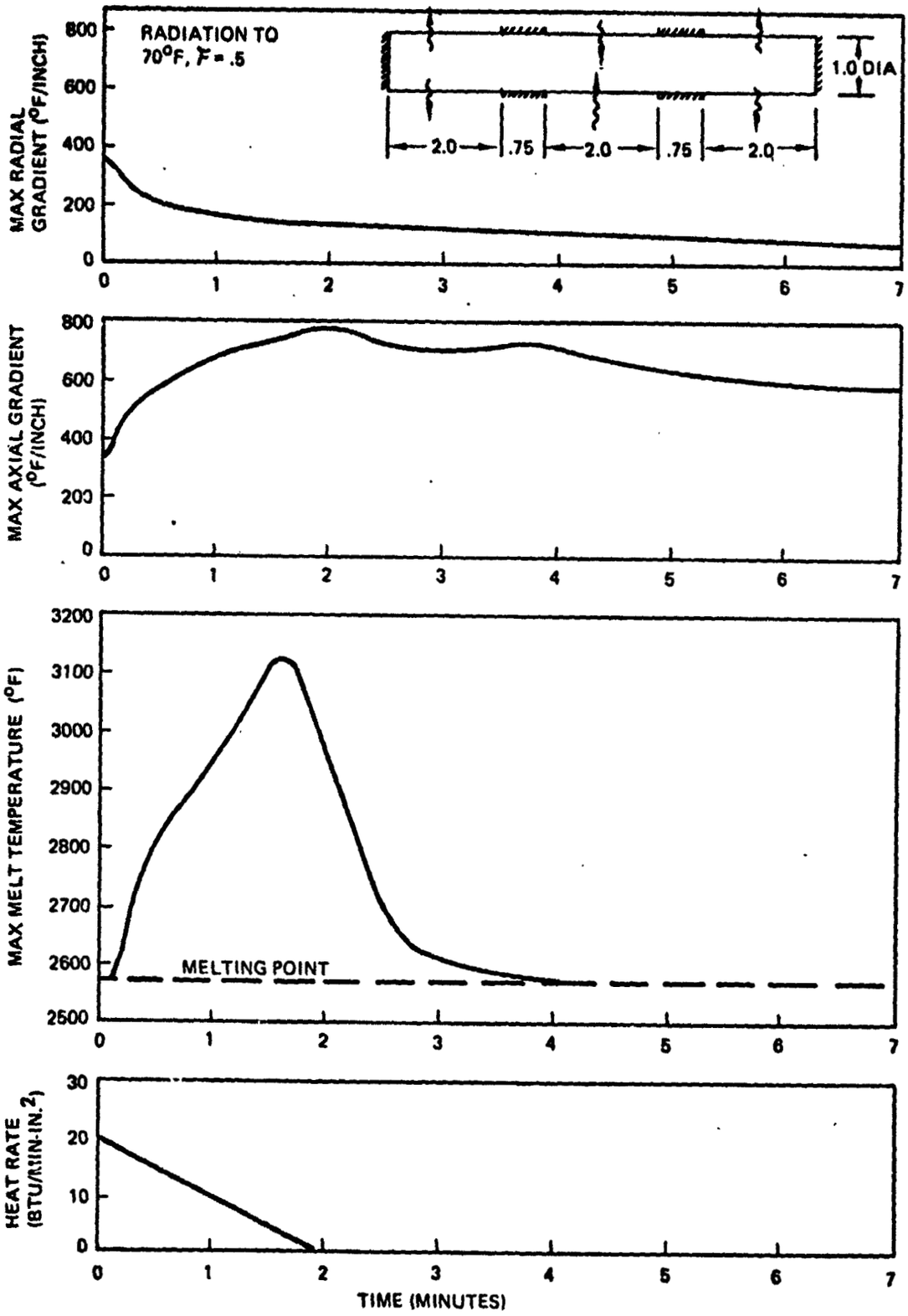

FIGURE 6

RUN 71 - TEMPERATURE GRADIENT & HEAT FLUX PROFILES

ORIGINAL PAGE IS
OF POOR QUALITY

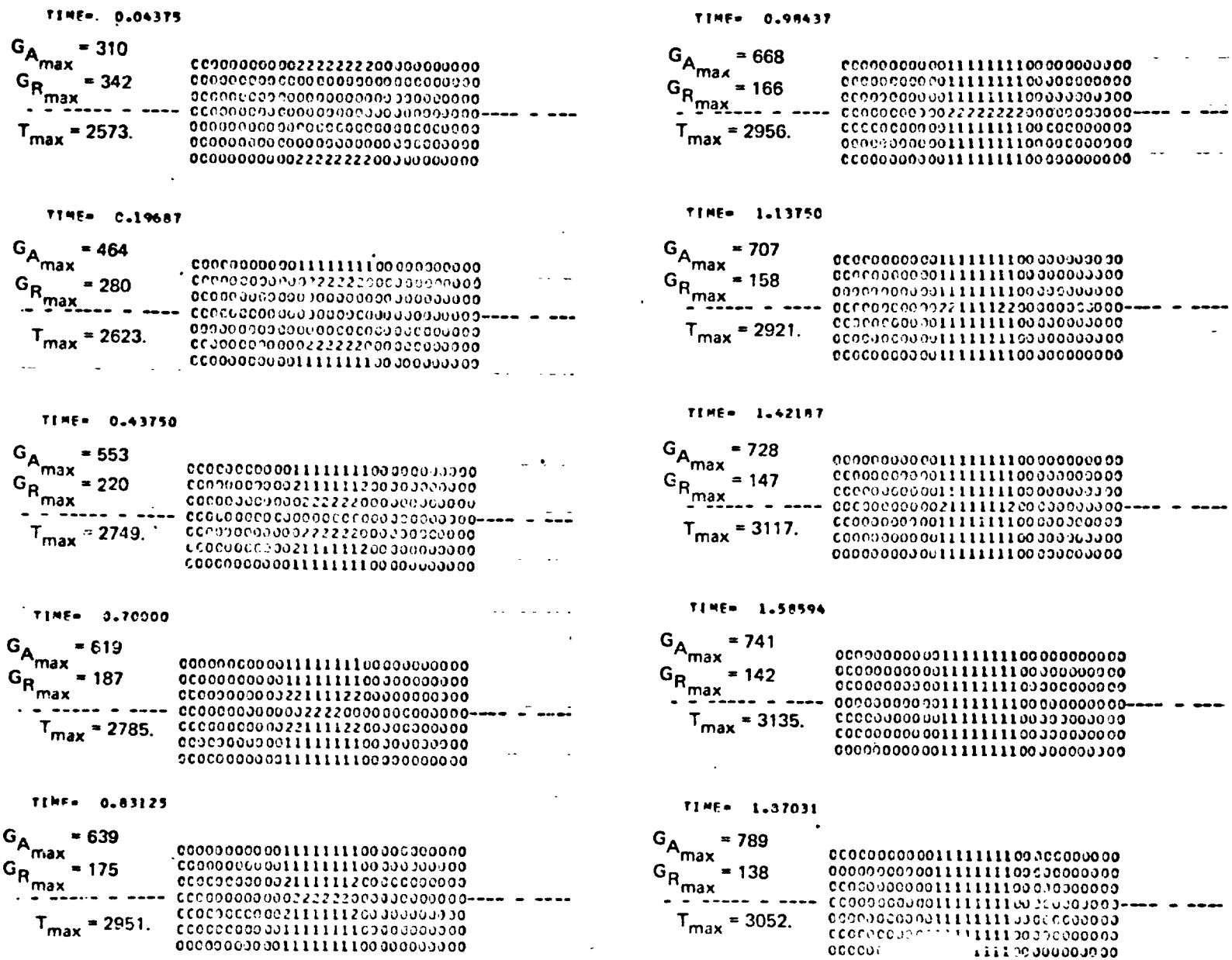

Figure 7. Run 71 - MELT ZONES

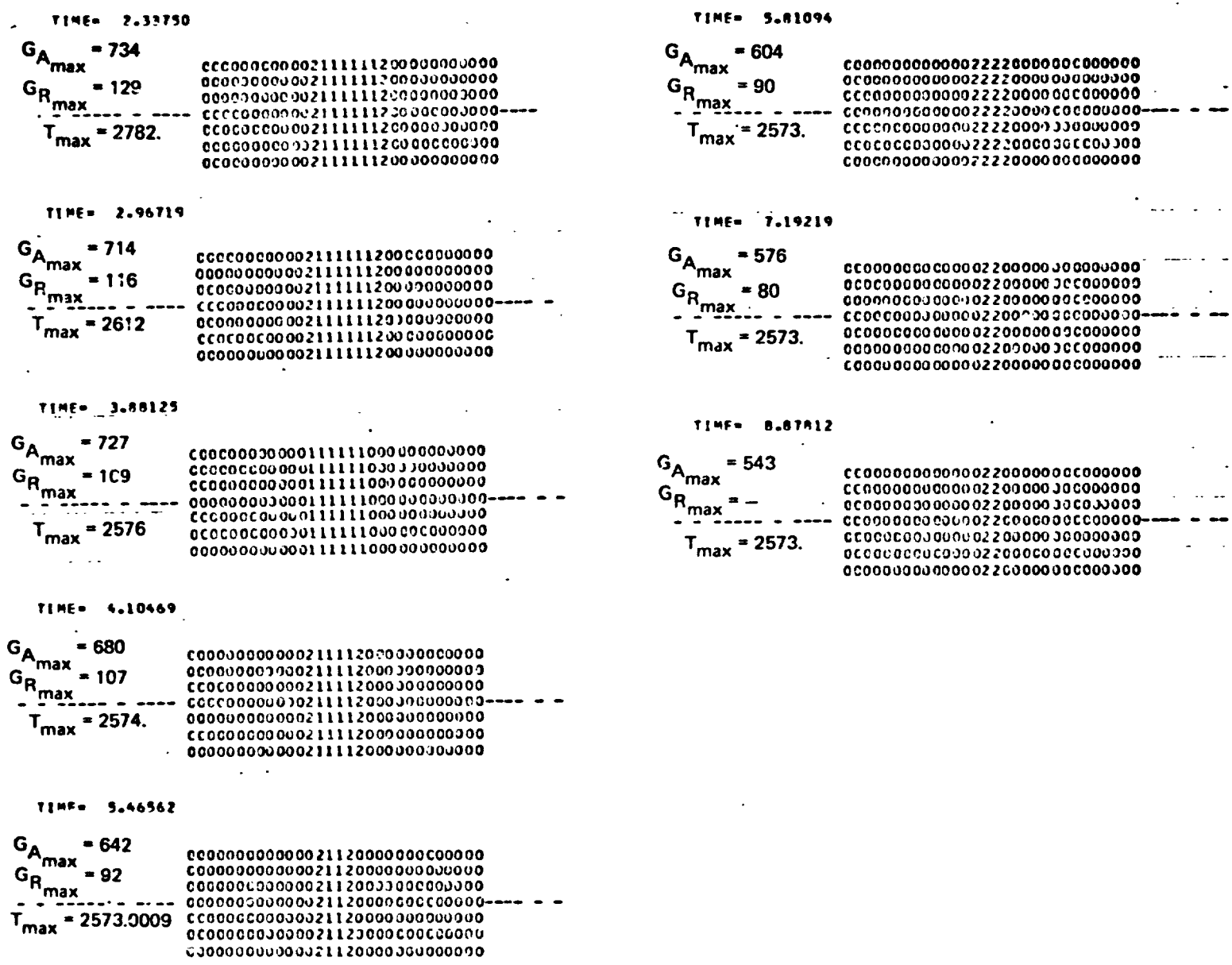

Figure 7 Run 71 (Continued)

ORIGINAL PAGE IS
OF POOR QUALITY

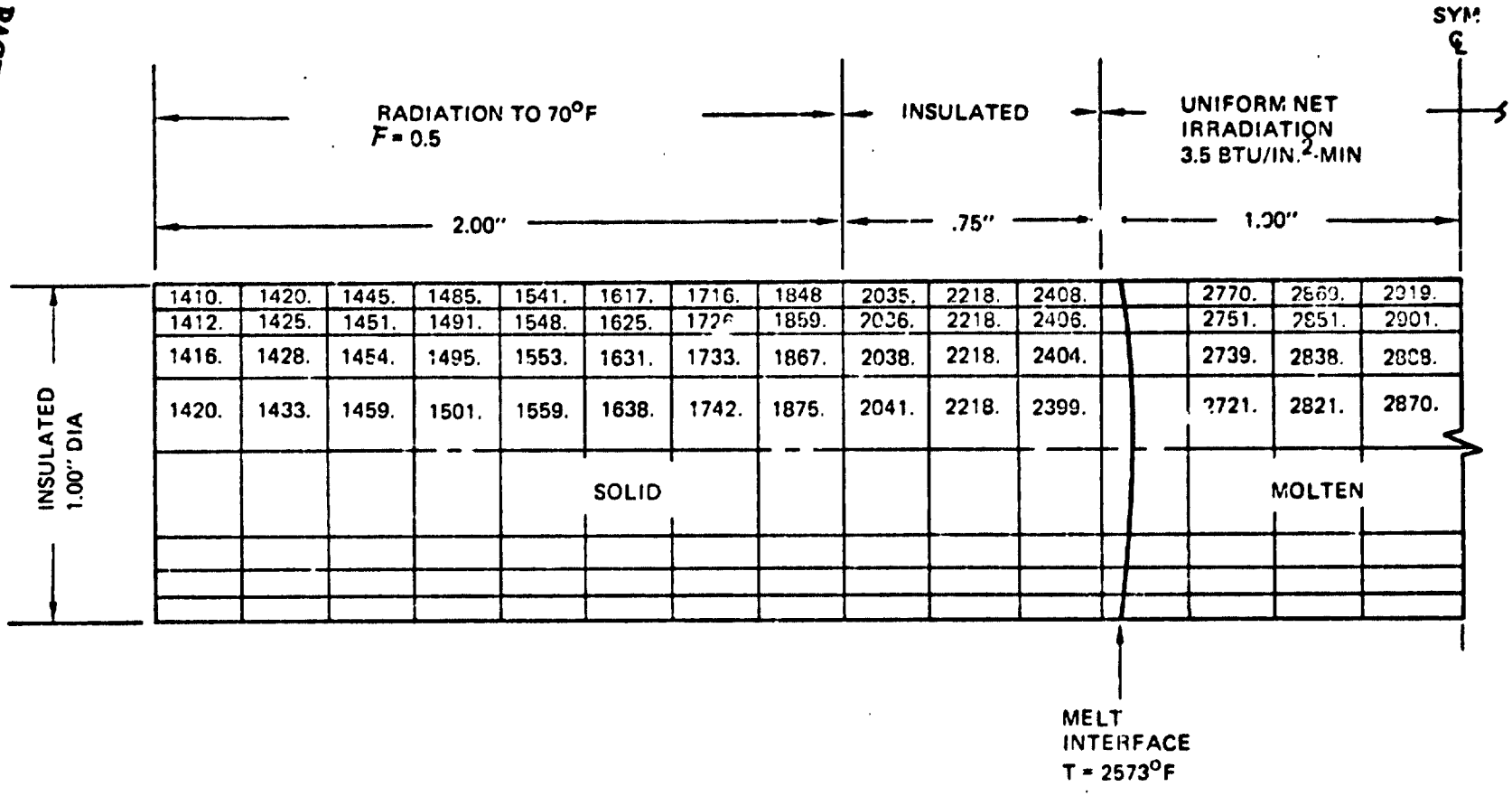

Figure 8. Run 75 STEADY STATE–NO CONVECTION

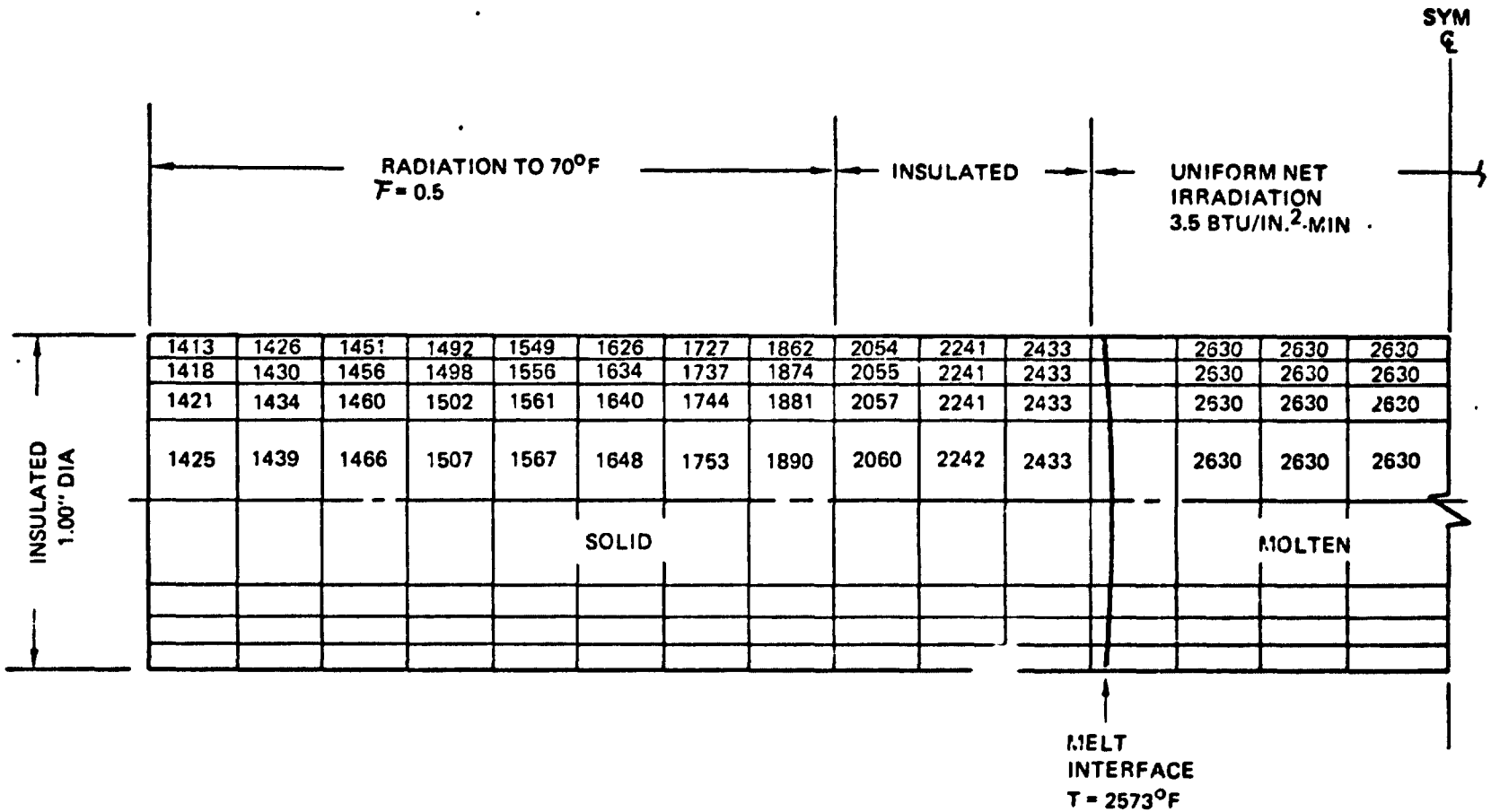

Figure 9. Run 82 STEADY STATE–INFINITE CONVECTION

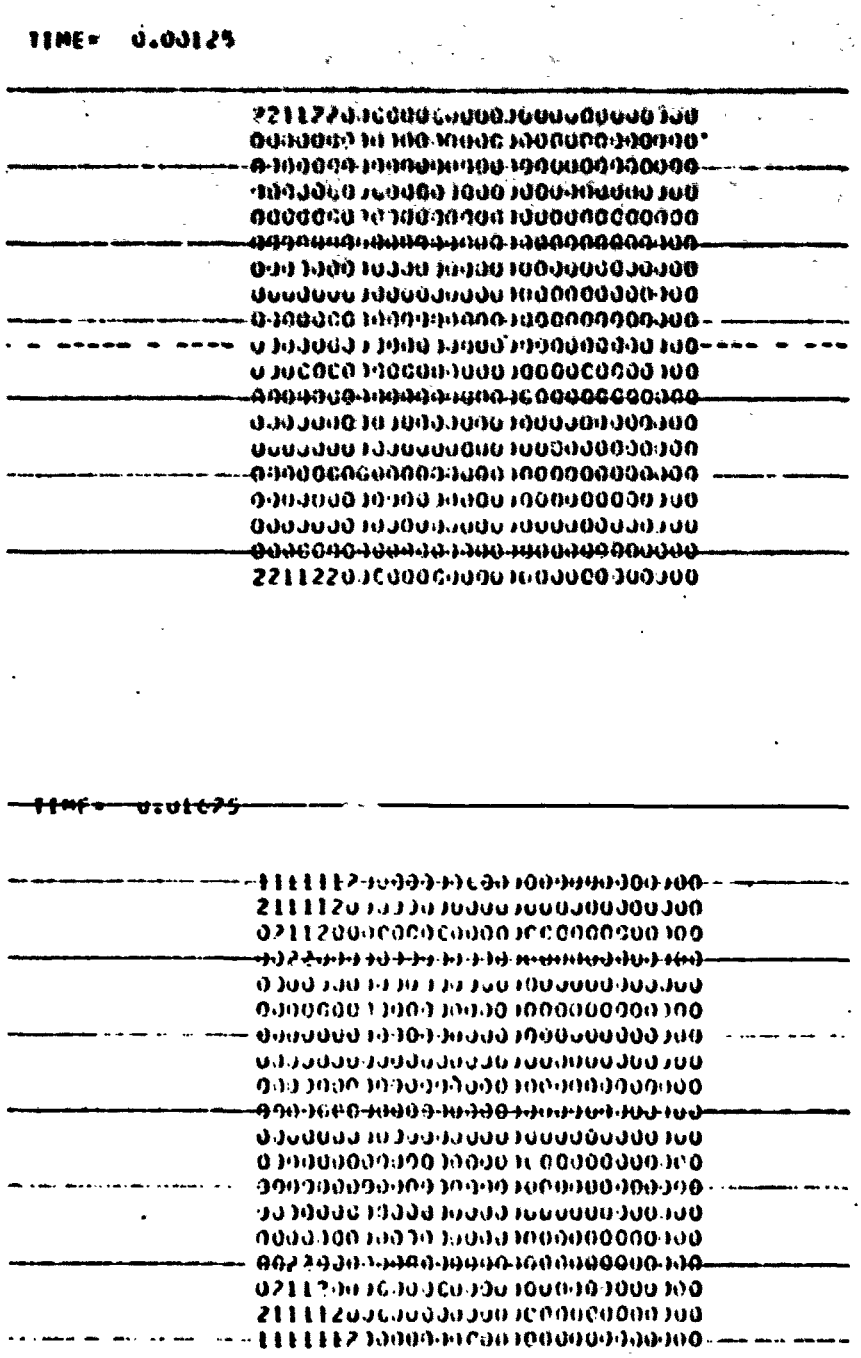

ORIGINAL PAGE IS
OF POOR QUALITY

FIGURE: 10 . *Run 29* - MELT ZONES

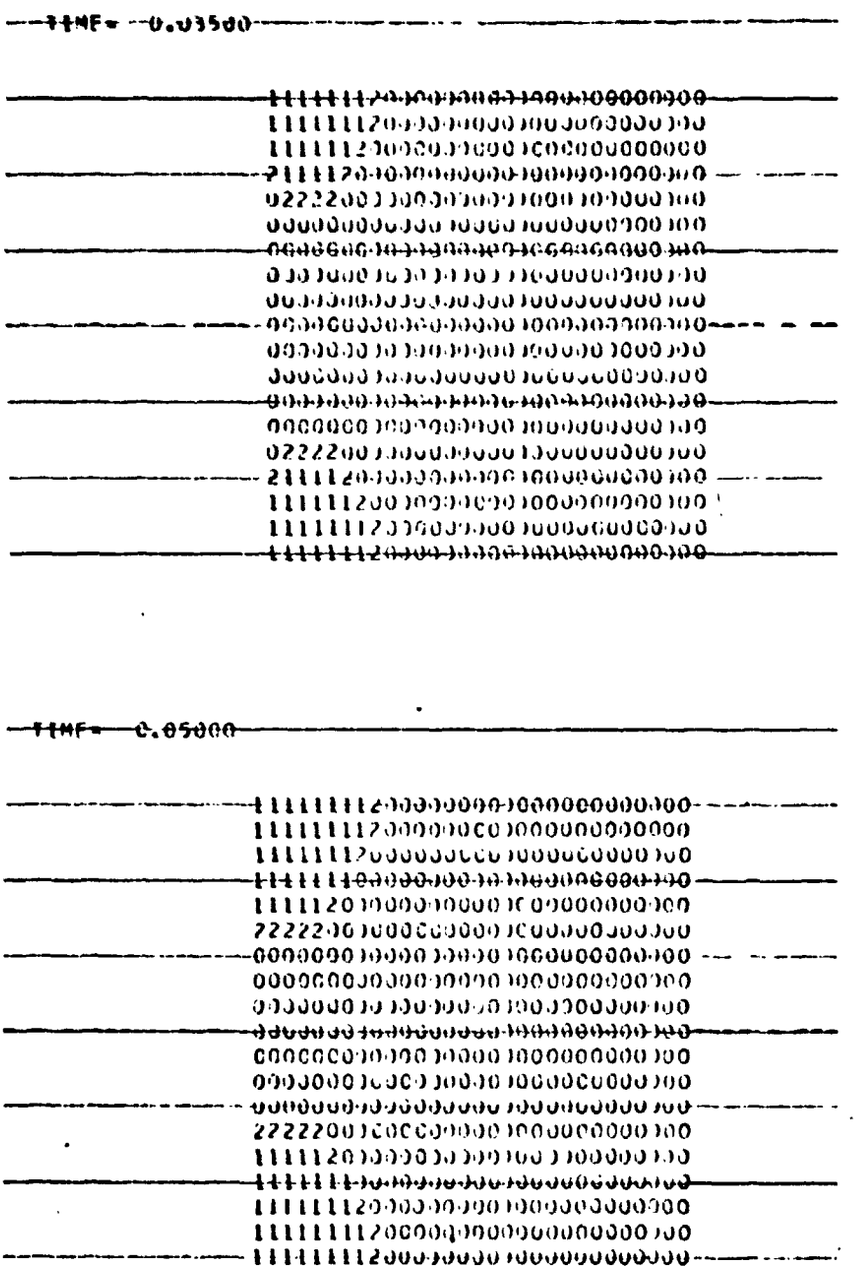

Figure 10. Run 29 (Continued)

ORIGINAL PAGE IS
OF POOR QUALITY

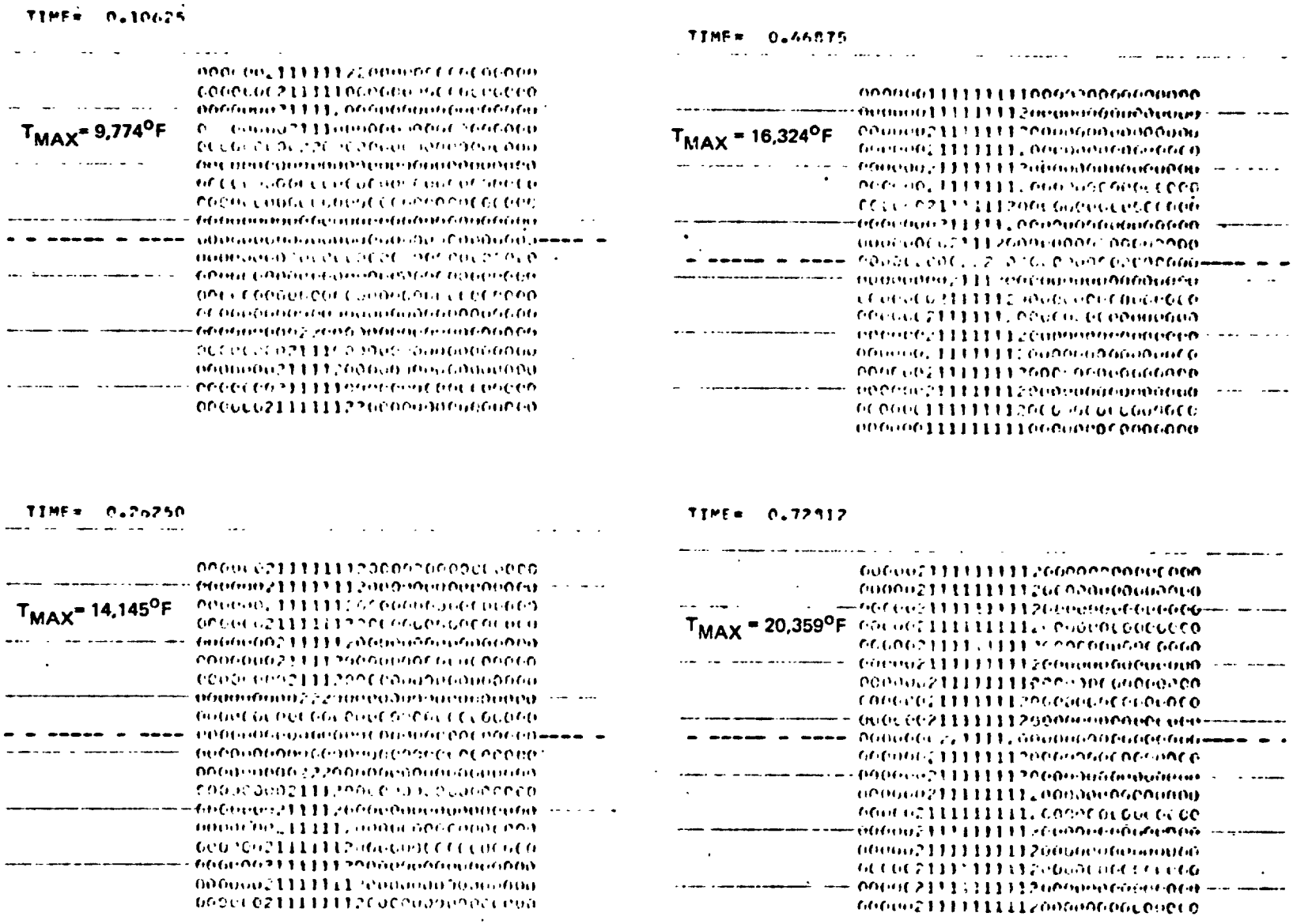

FIGURE: 11 . *Run 36* . - MELT ZONES

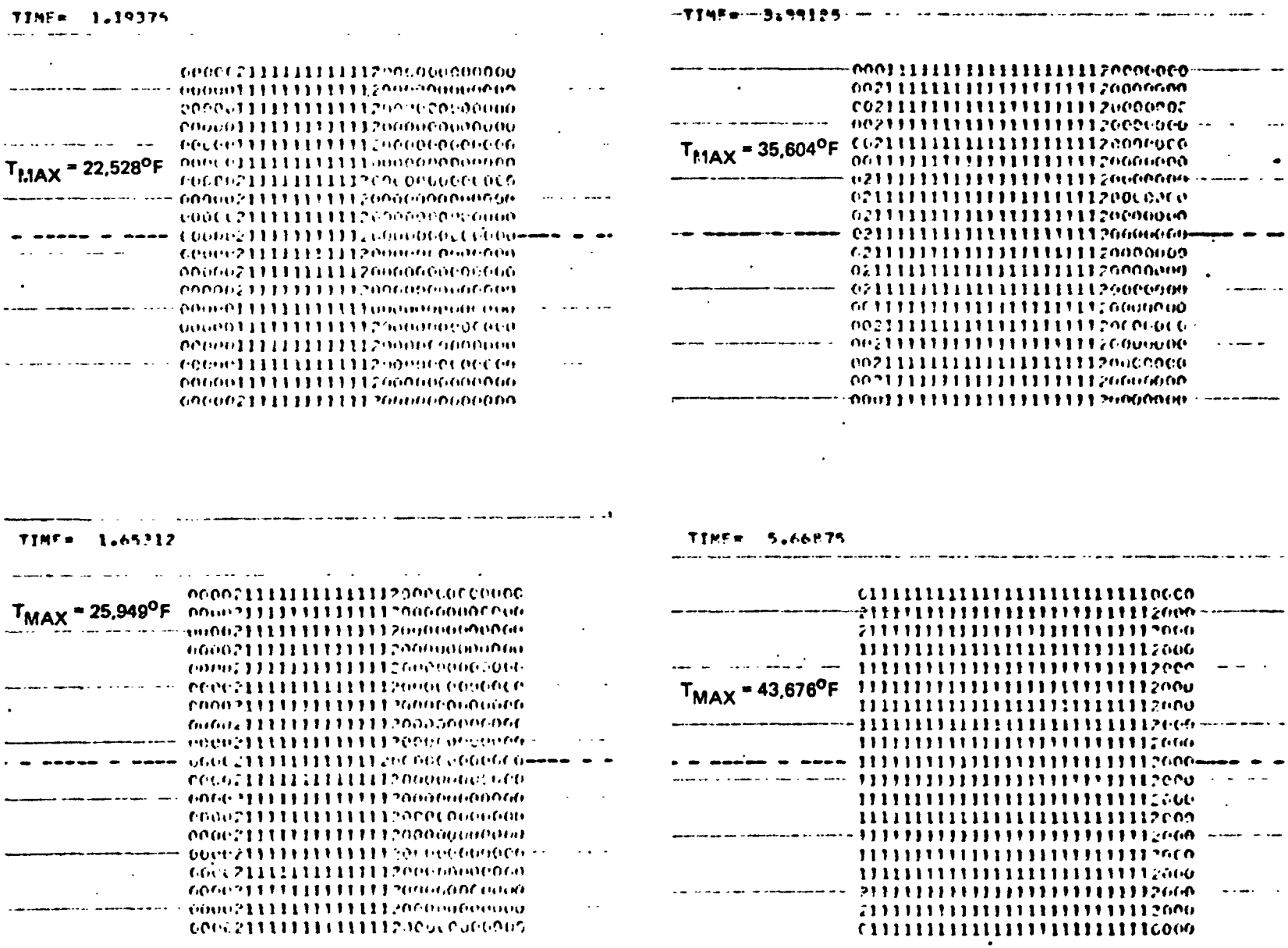

FIGURE 11. *Run 36 (Continued)*

ORIGINAL PAGE IS
OF POOR QUALITY

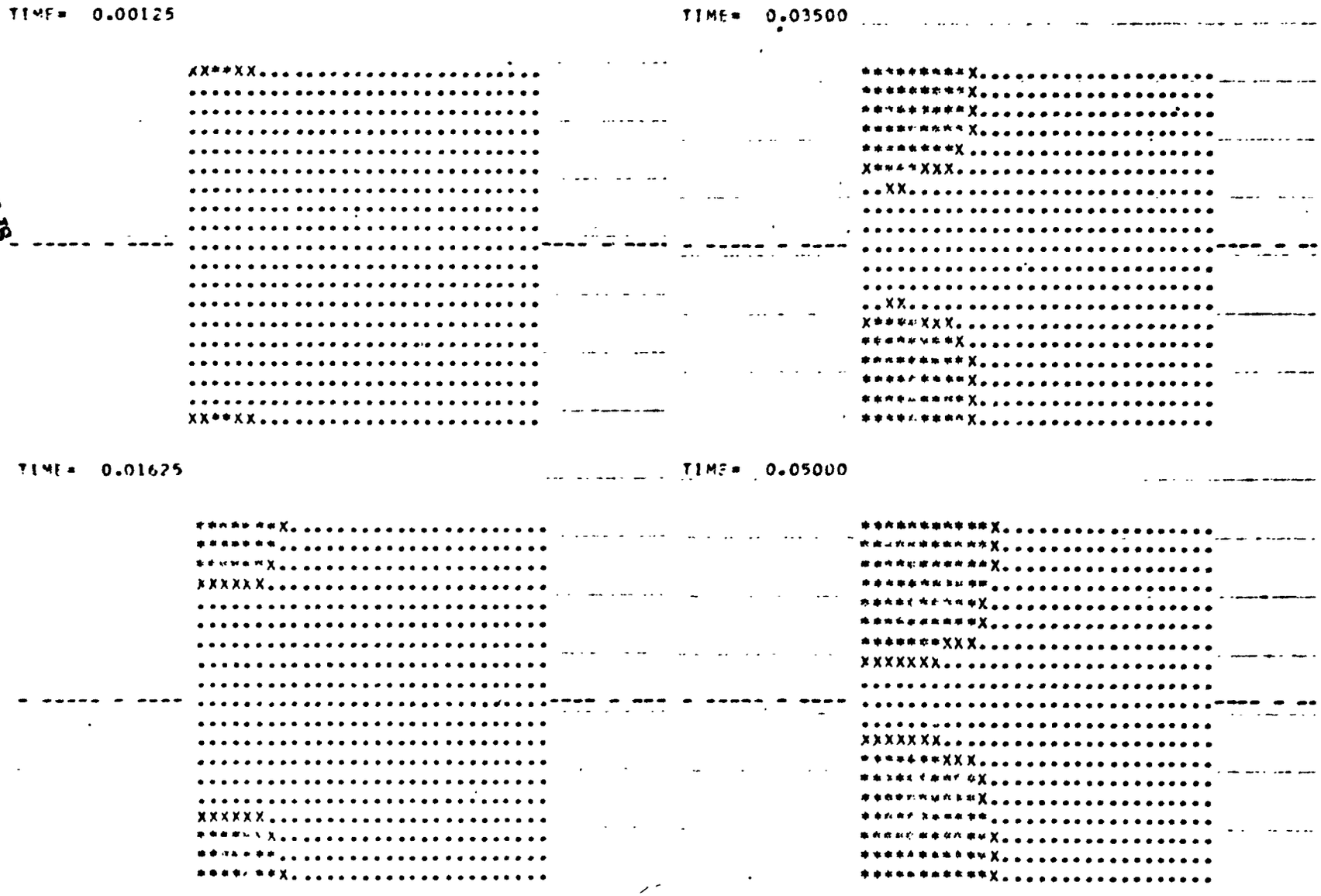

FIGURE: 12 *Run 39* - MELT ZONES

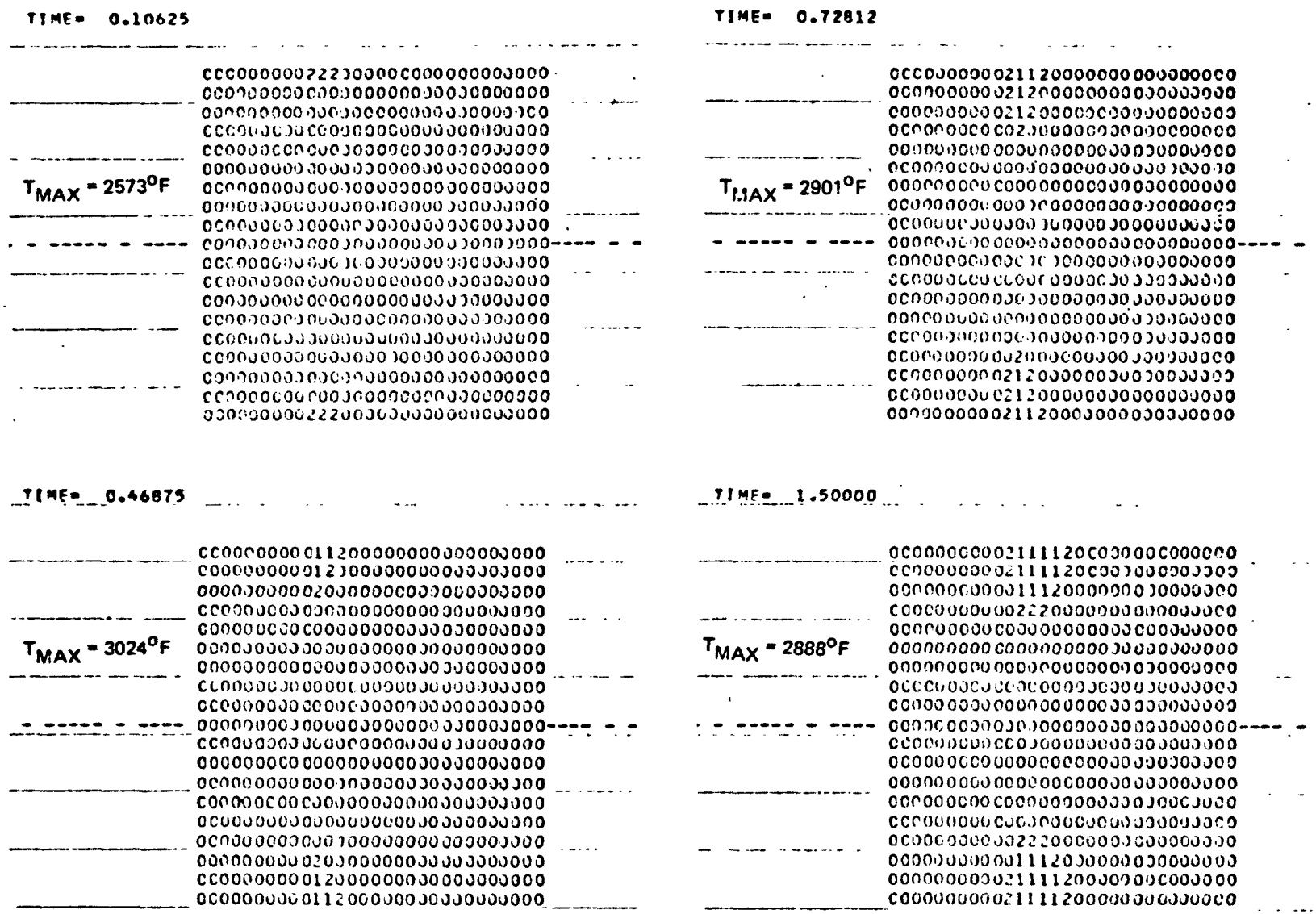

FIGURE: 13 *Run 40* - MELT ZONES

ORIGINAL PAGE IS
OF POOR QUALITY

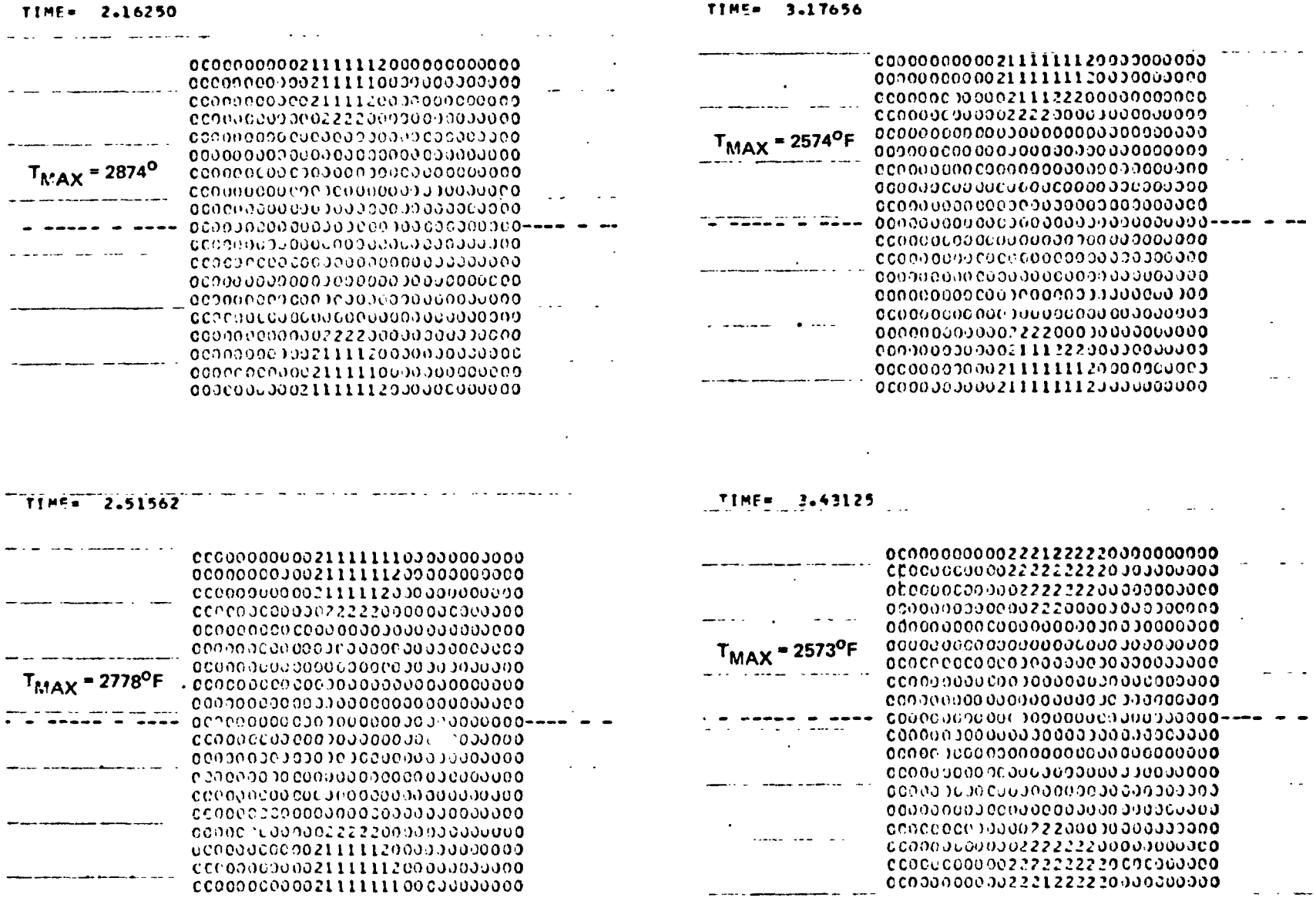

FIGURE: 13 . *Run 40 (Continued)*

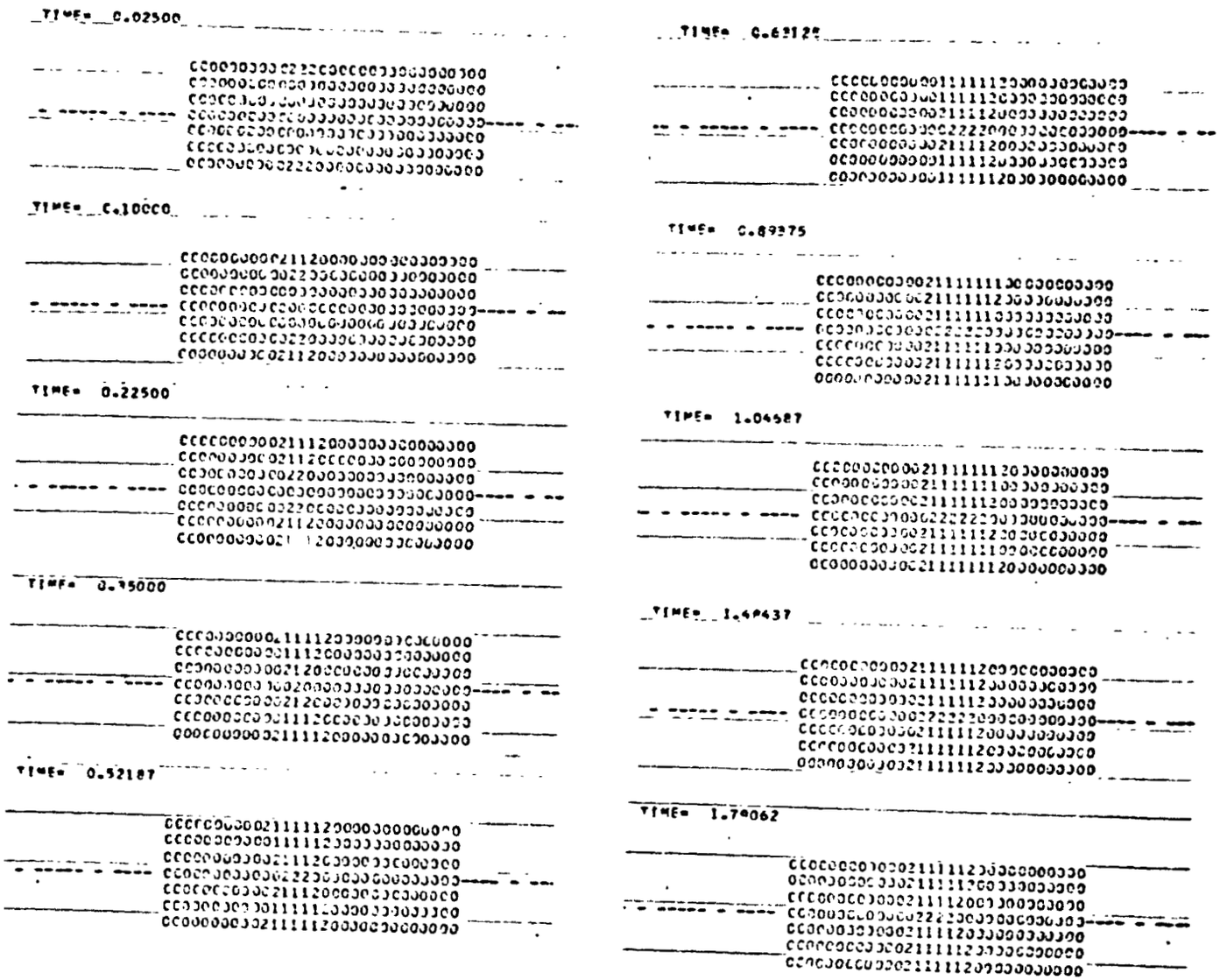

FIGURE: 14 . *Run 44* - MELT ZONES

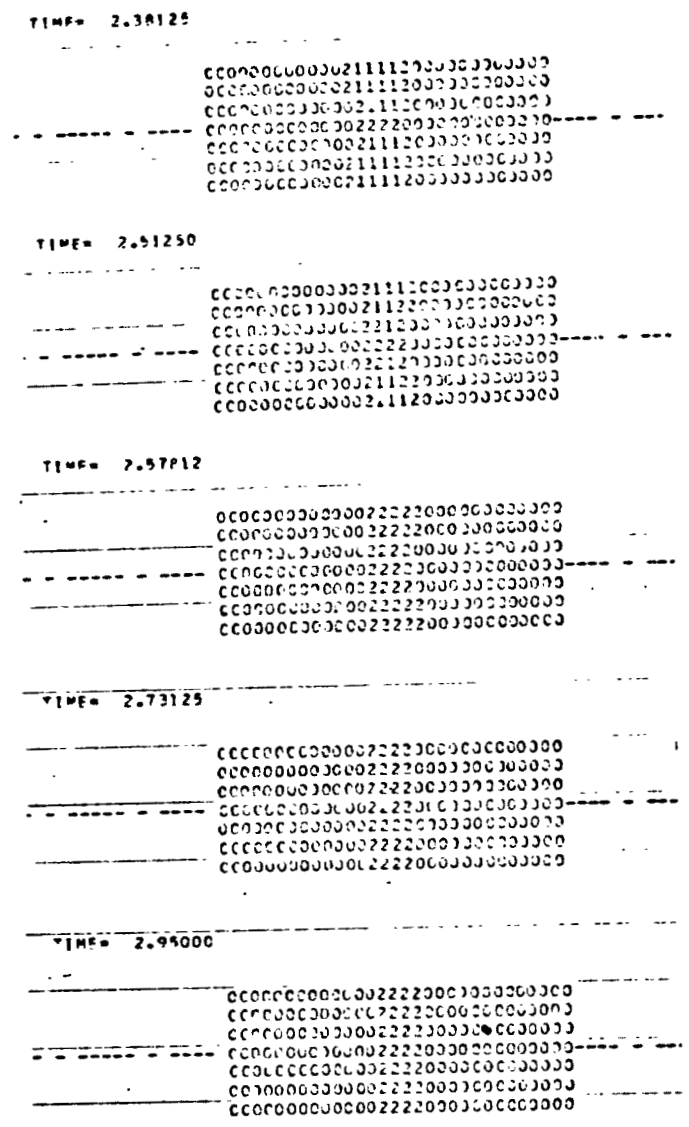

Figure 14. Run 44 (Continued)

ORIGINAL PAGE IS
OF POOR QUALITY

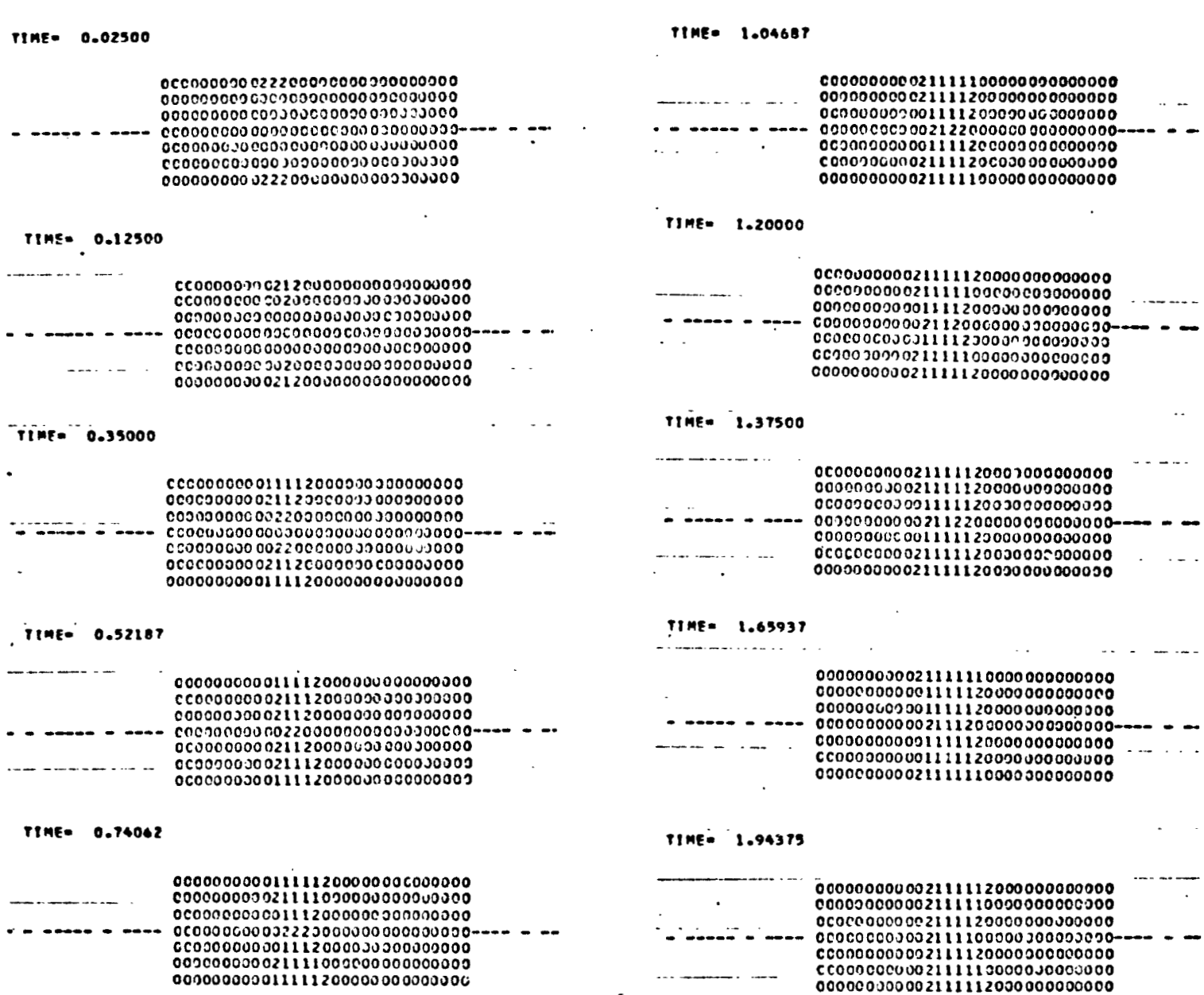

Figure 15. *Run 49* - MELT ZONES

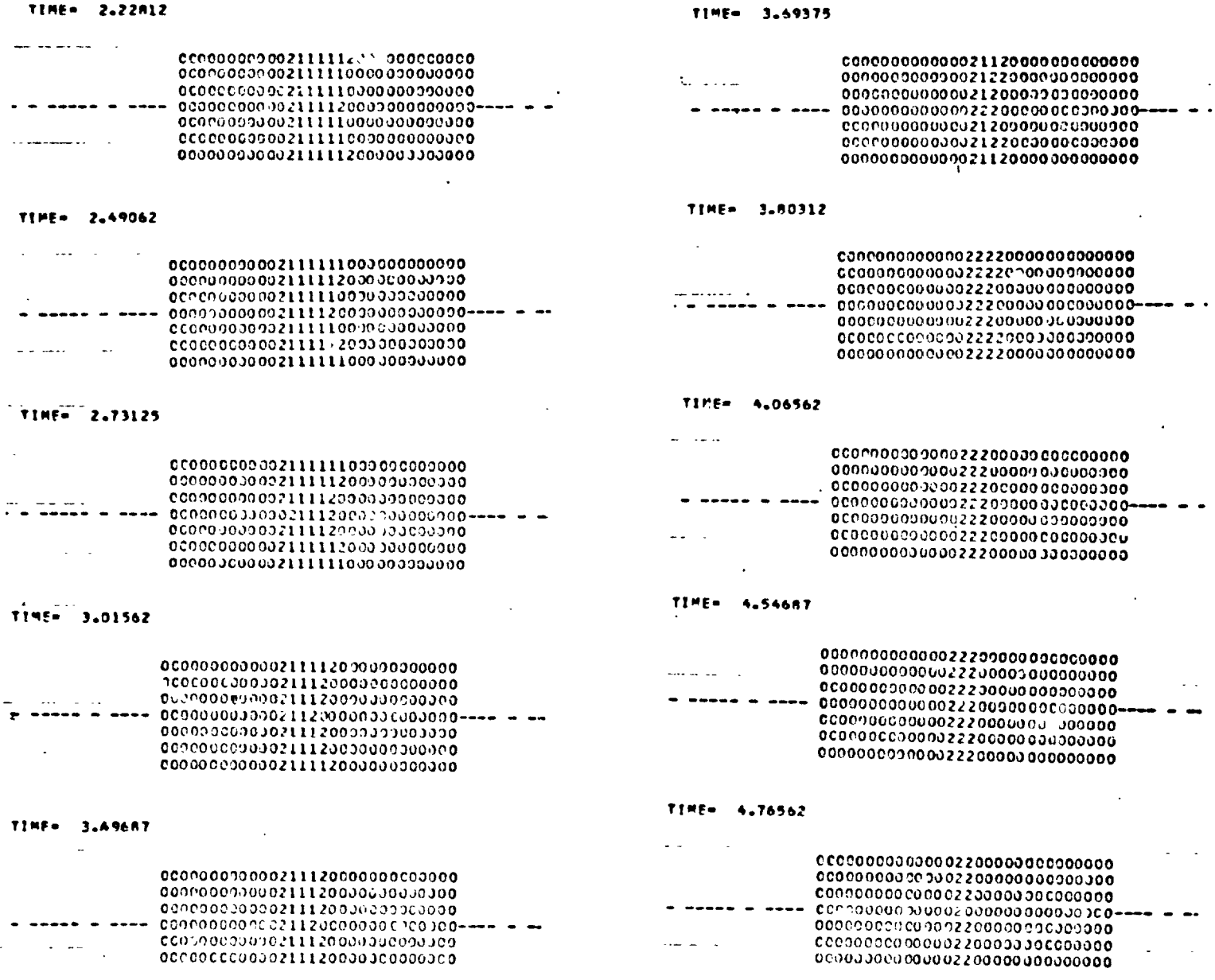

Figure 15. Run 49 (Continued)

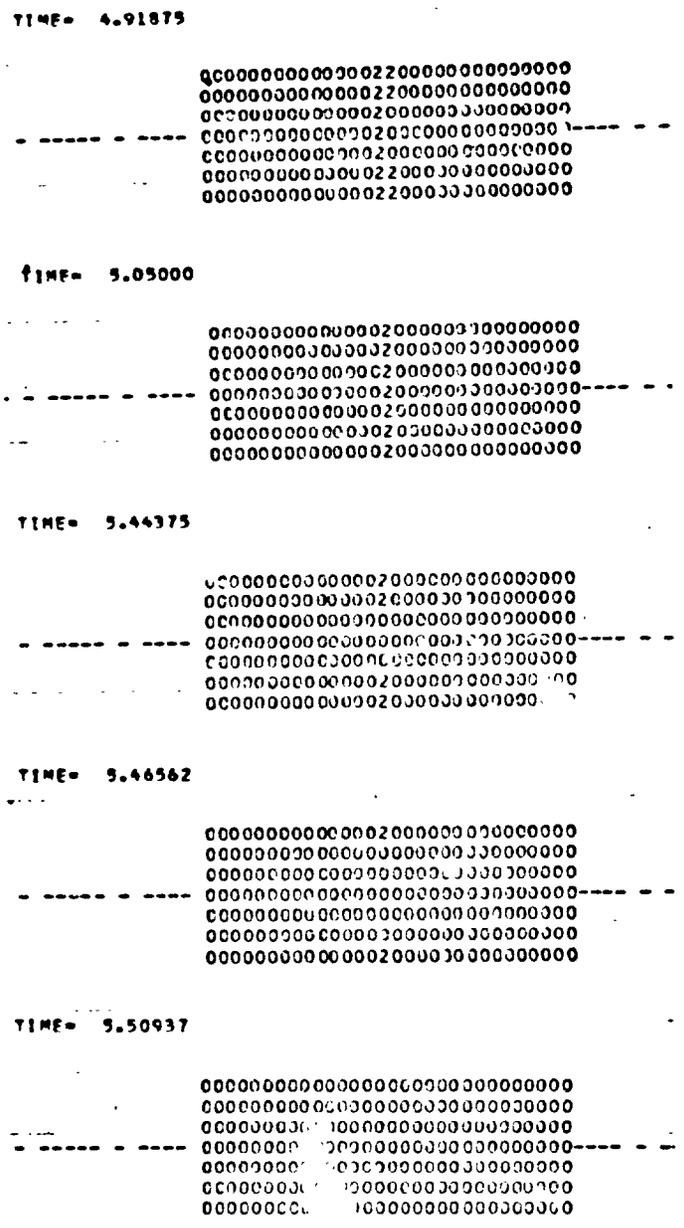

Figure 15. *Run 49 (Continued,*

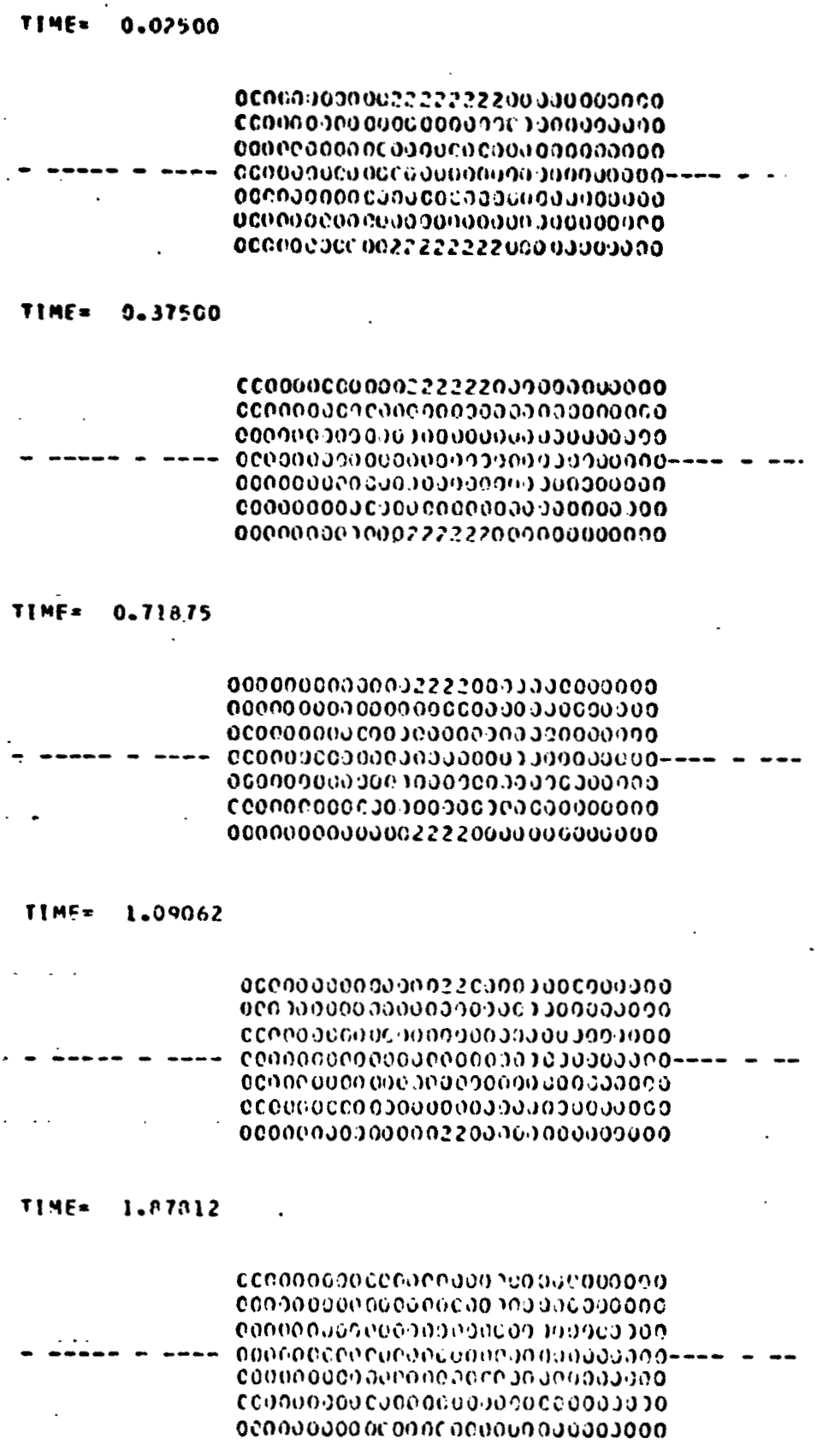

ORIGINAL PAGE IS
OF POOR QUALITY

Figure 16. *Run 55* - MELT ZONES

Figure 17. Run 56. - MELT ZONES

ORIGINAL PAGE IS
OF POOR QUALITY

Figure 17. Run 56 (Continued)

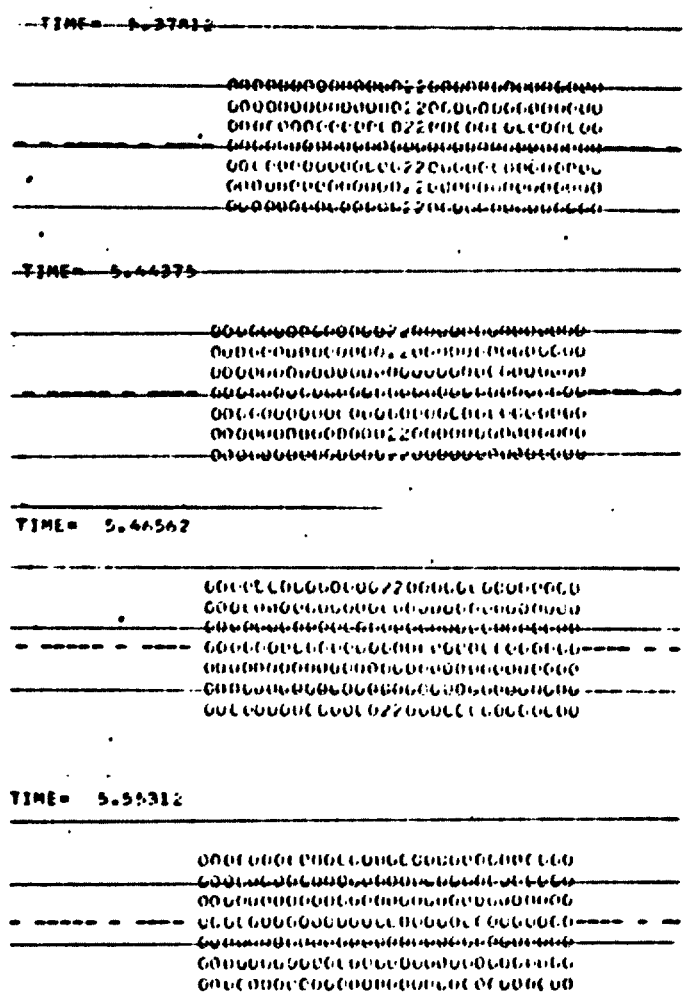

Figure 17. Run 56 (Continued)

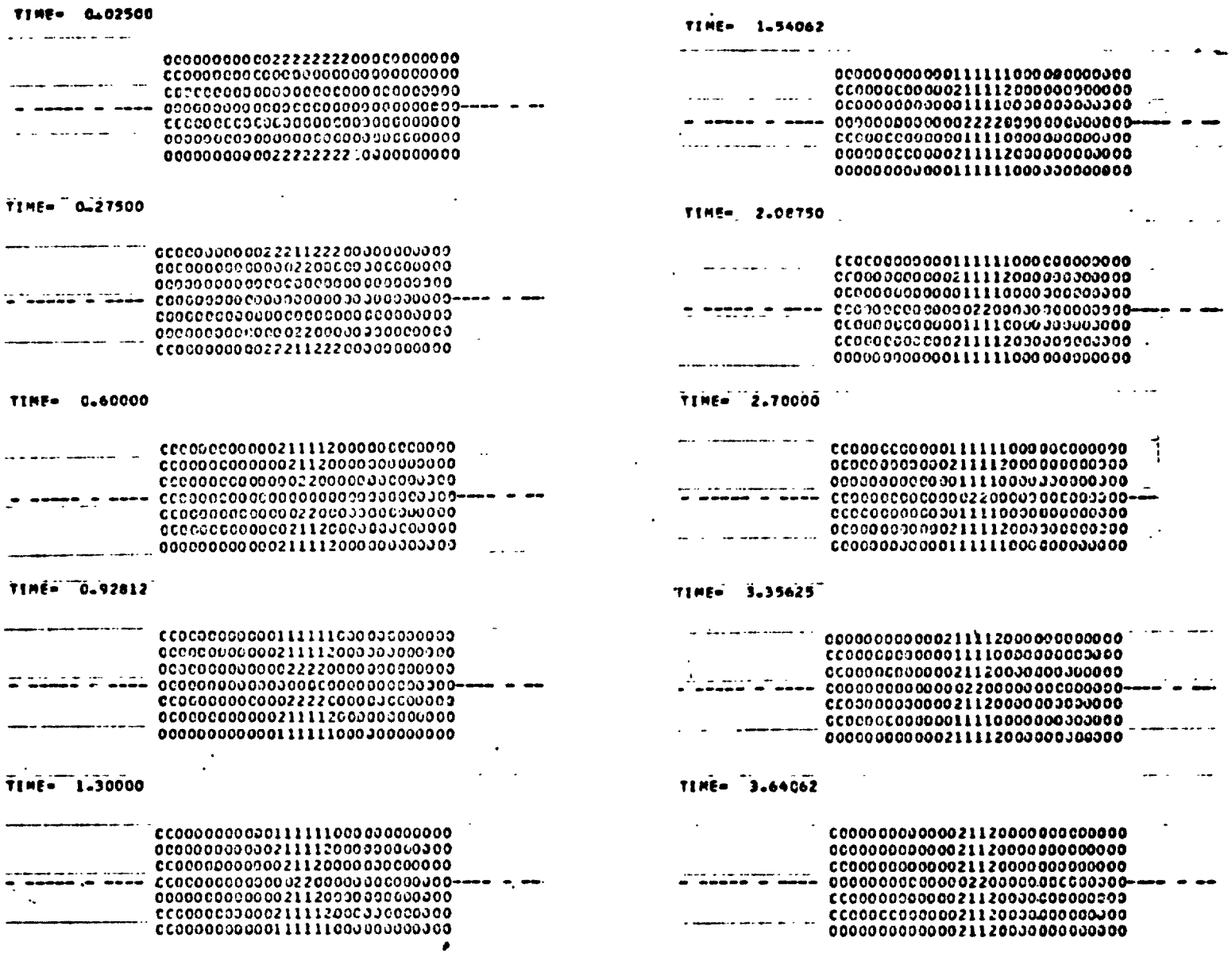

Figure 18. *Run 60* - MELT ZONES

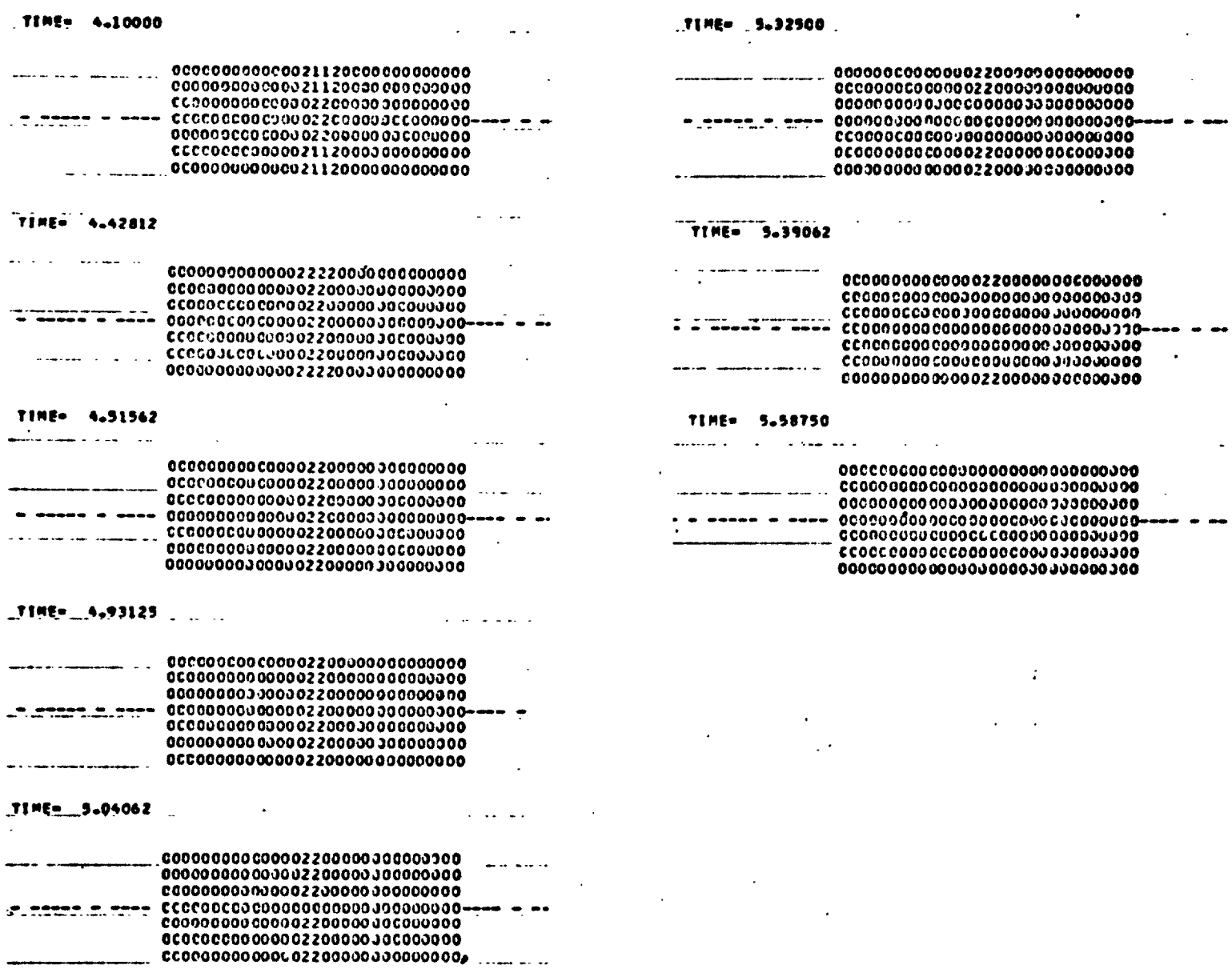

Figure 18. Run 60 (Continued)

ORIGINAL PAGE IS
OF POOR QUALITY

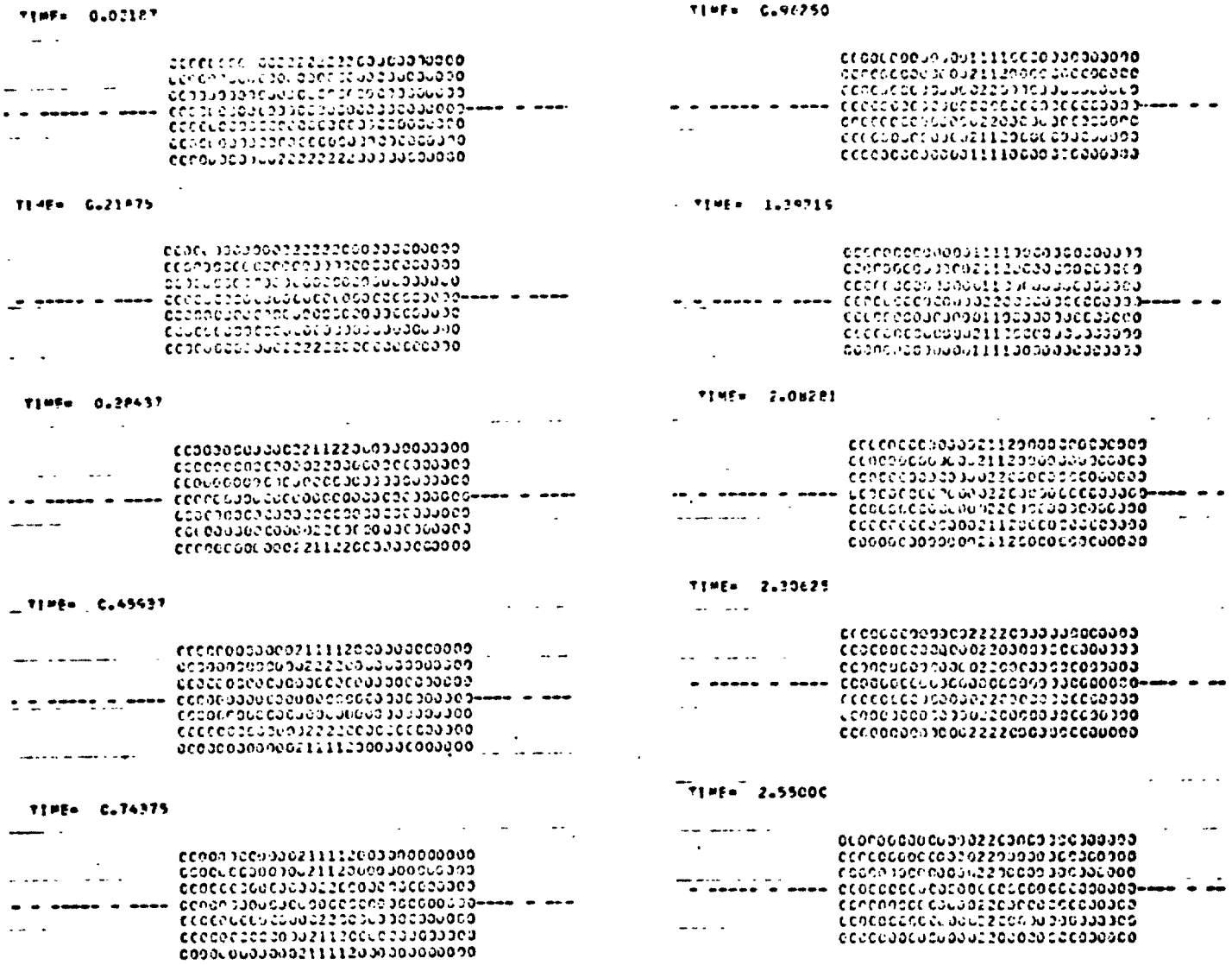

Figure 19. Run 62. - MELT ZONES

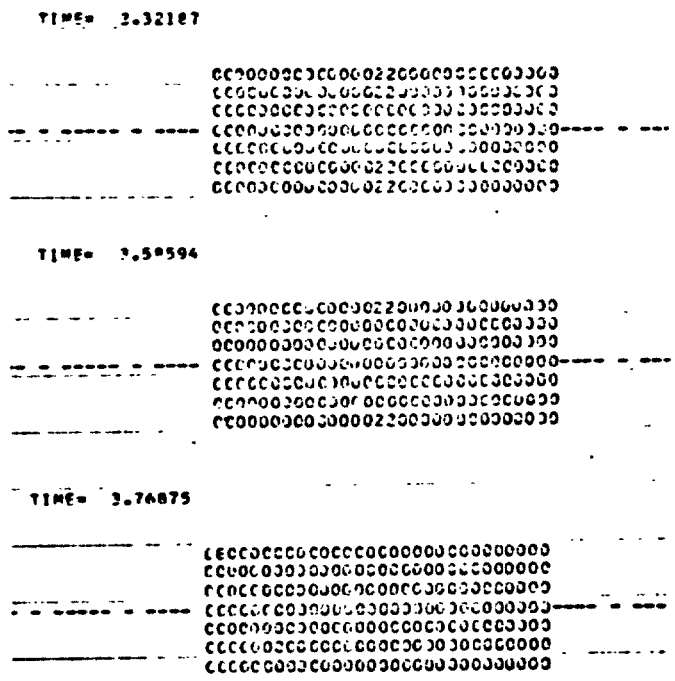

Figure 19. Run 62 (Continued)

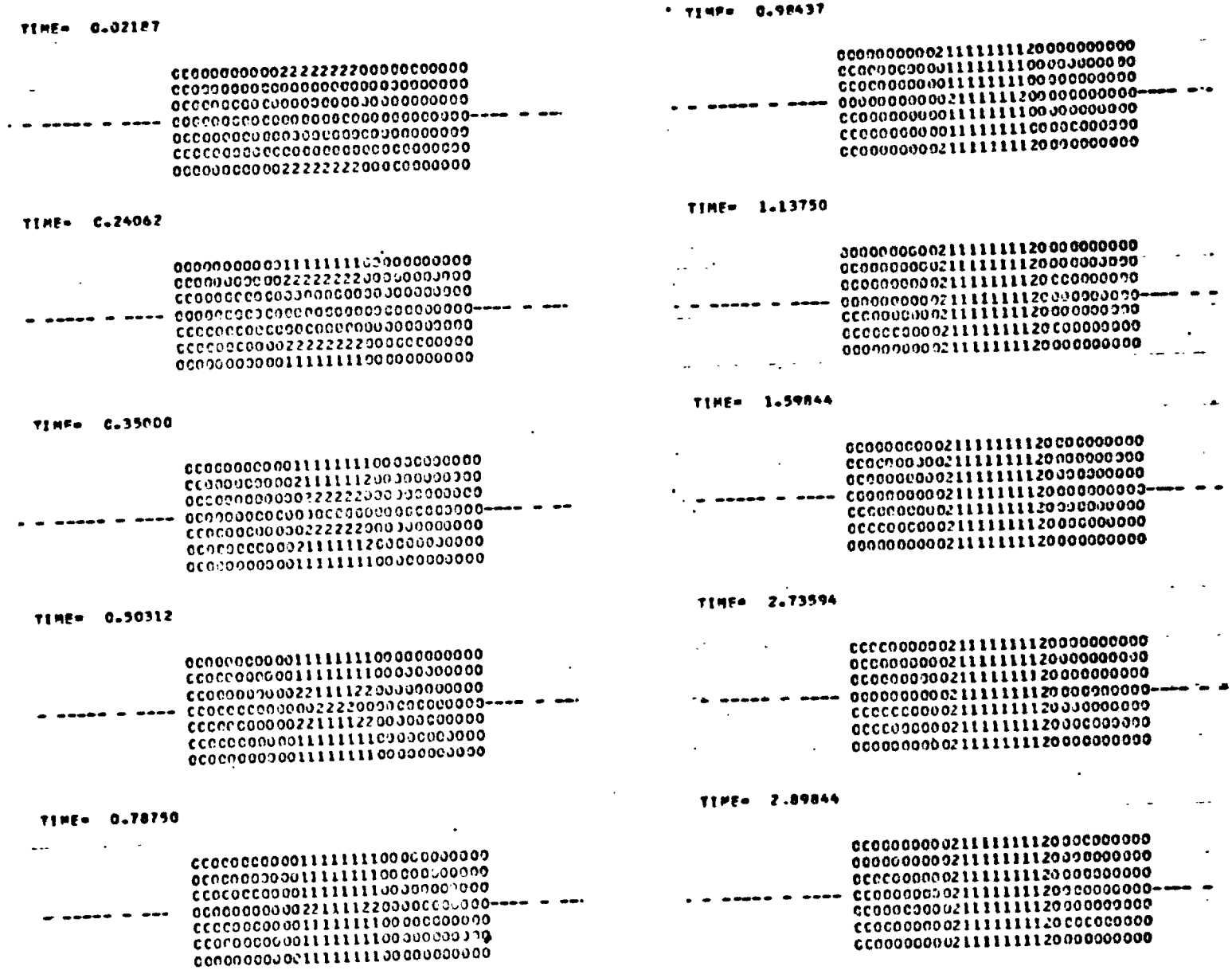

Figure 20. Run 65 - MELT ZONES

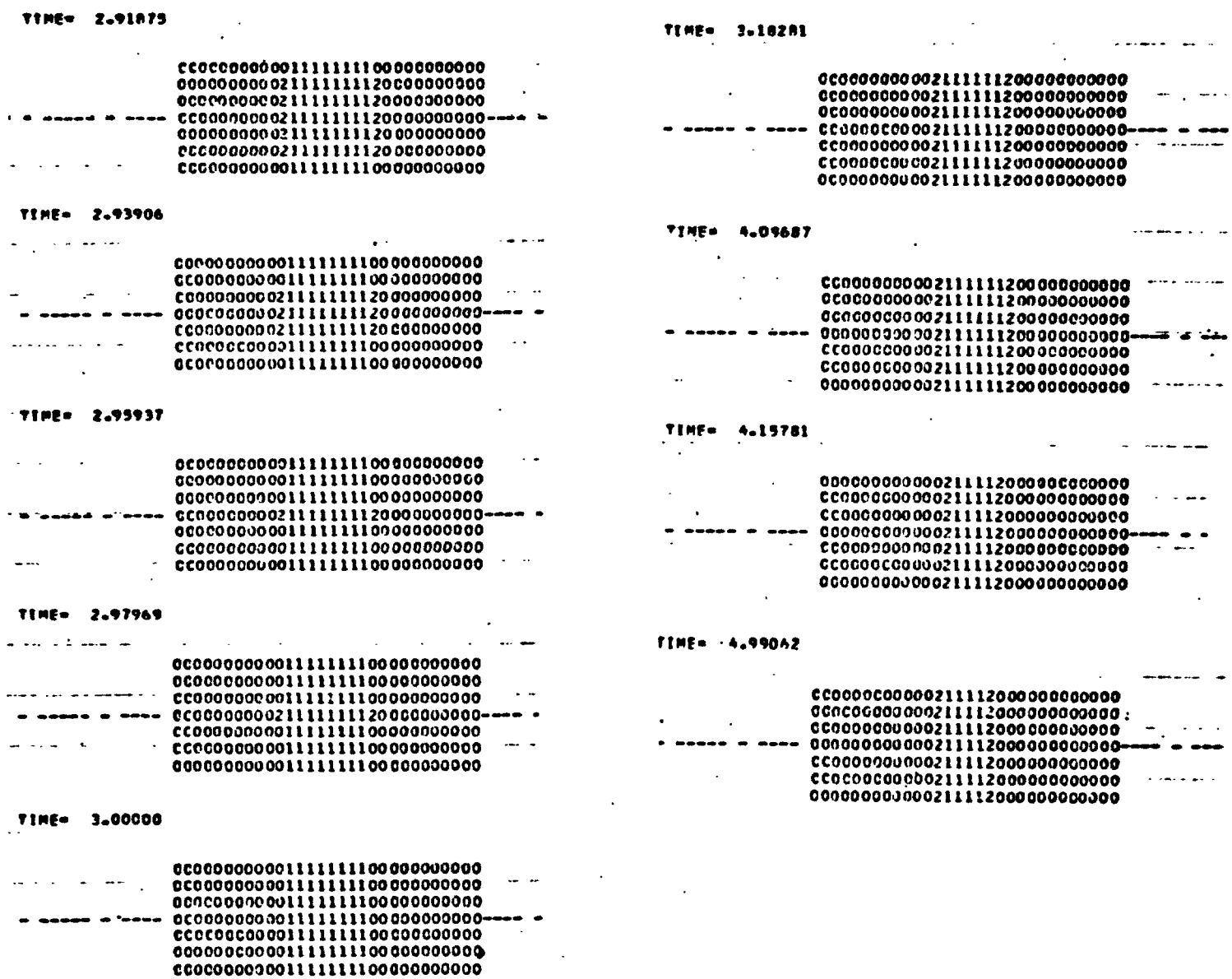

Figure 20. Run 65 (Continued)

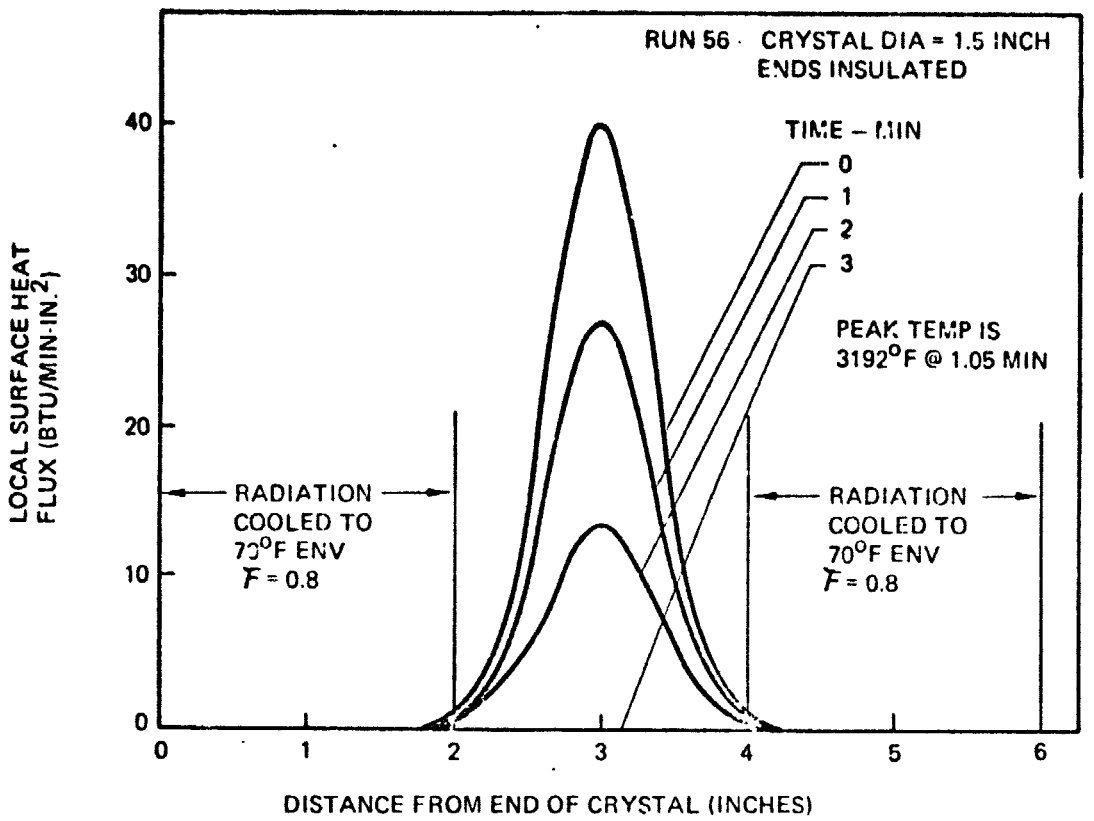

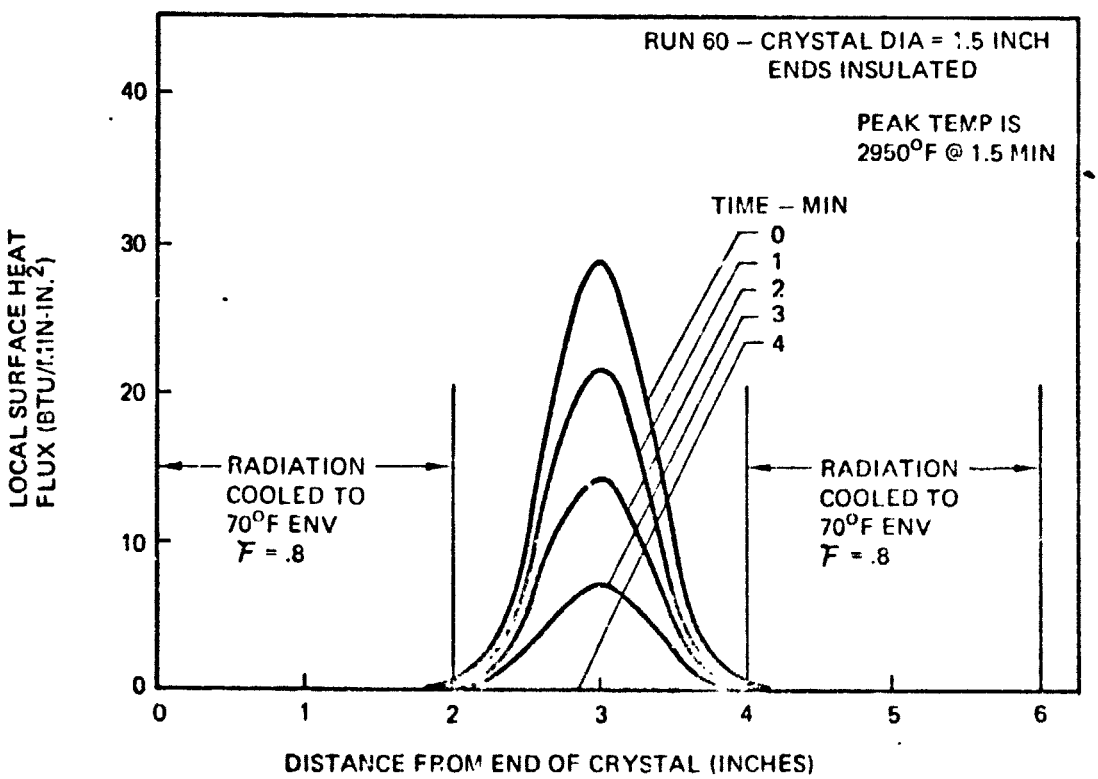

Figure 21

SURFACE HEAT FLUX RUN 56 & 60

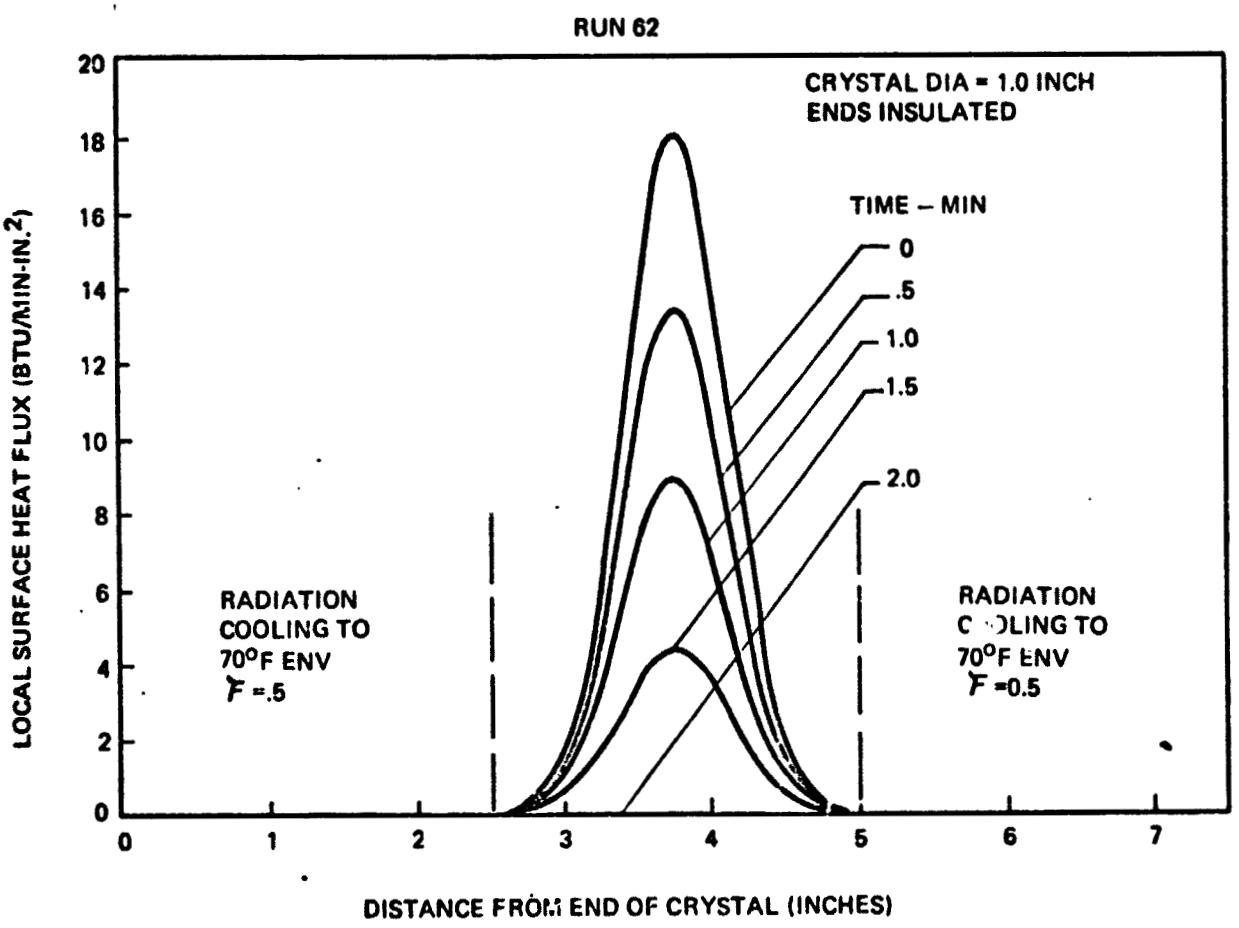

Figure 22

SURFACE HEAT FLUX RUN 62

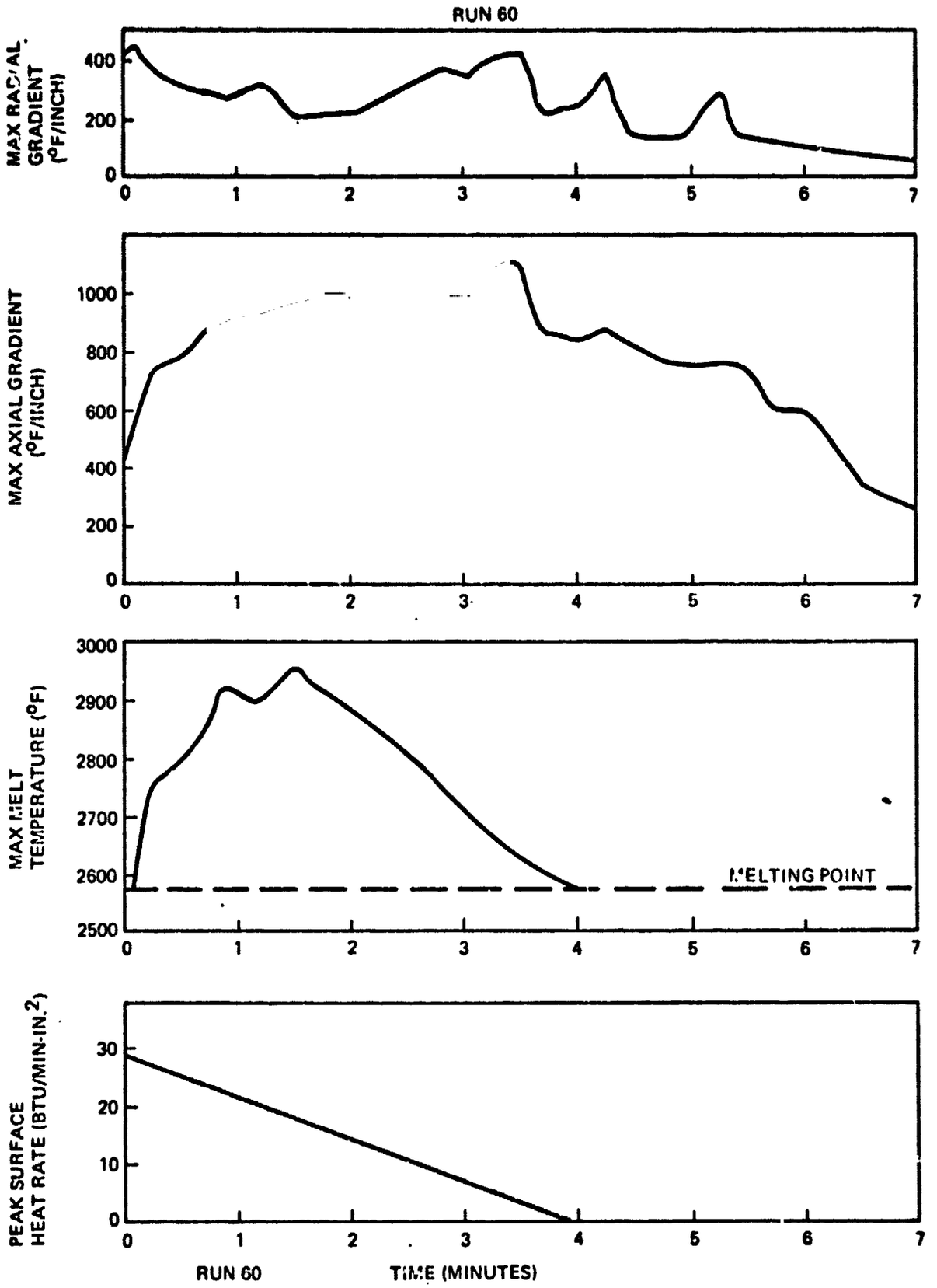

Figure 23
RUN 60 - TEMPERATURE GRADIENT & HEAT FLUX PROFILES

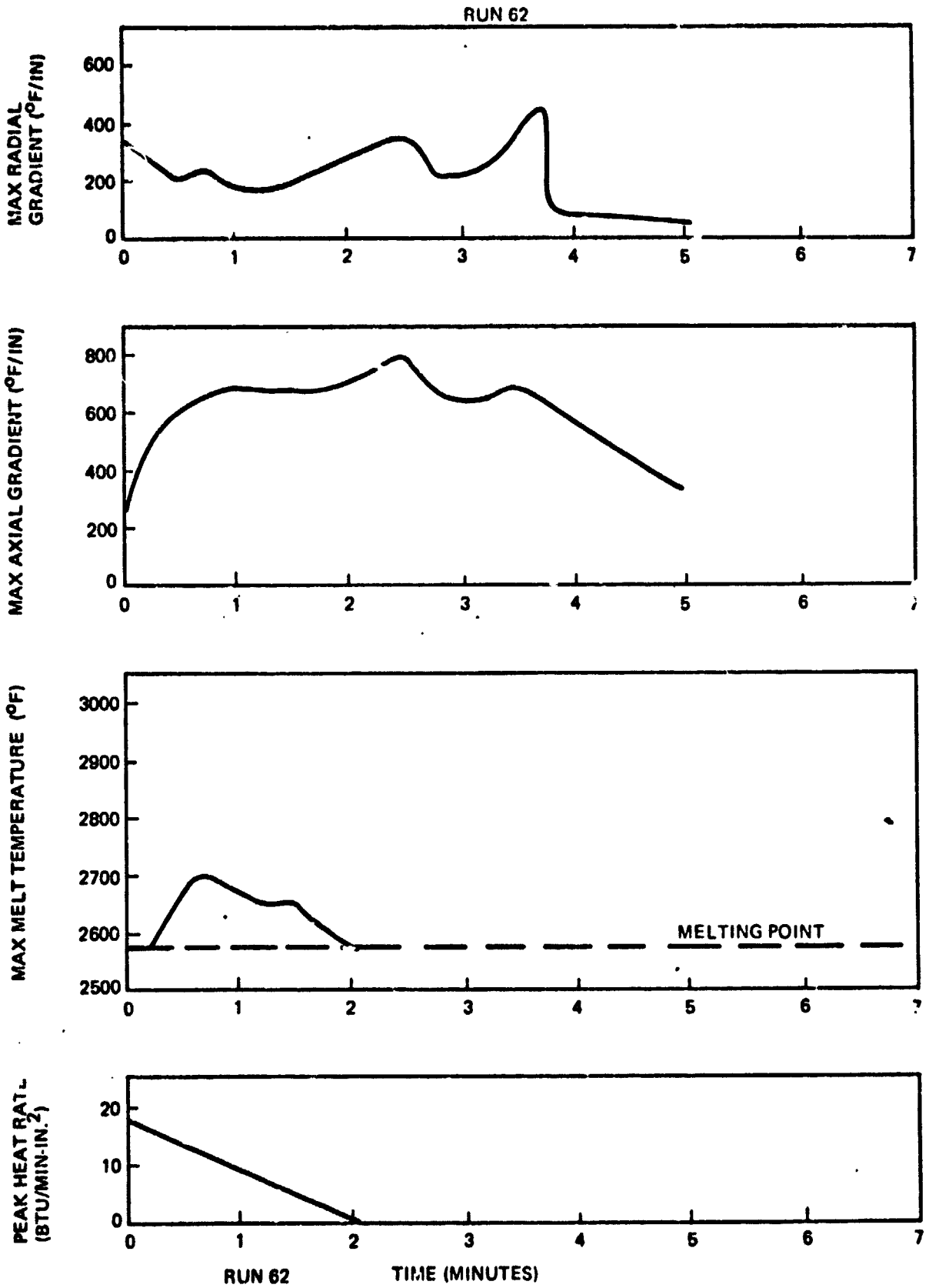

Figure 24

RUN 62 - TEMPERATURE GRADIENT & HEAT FLUX PROFILES

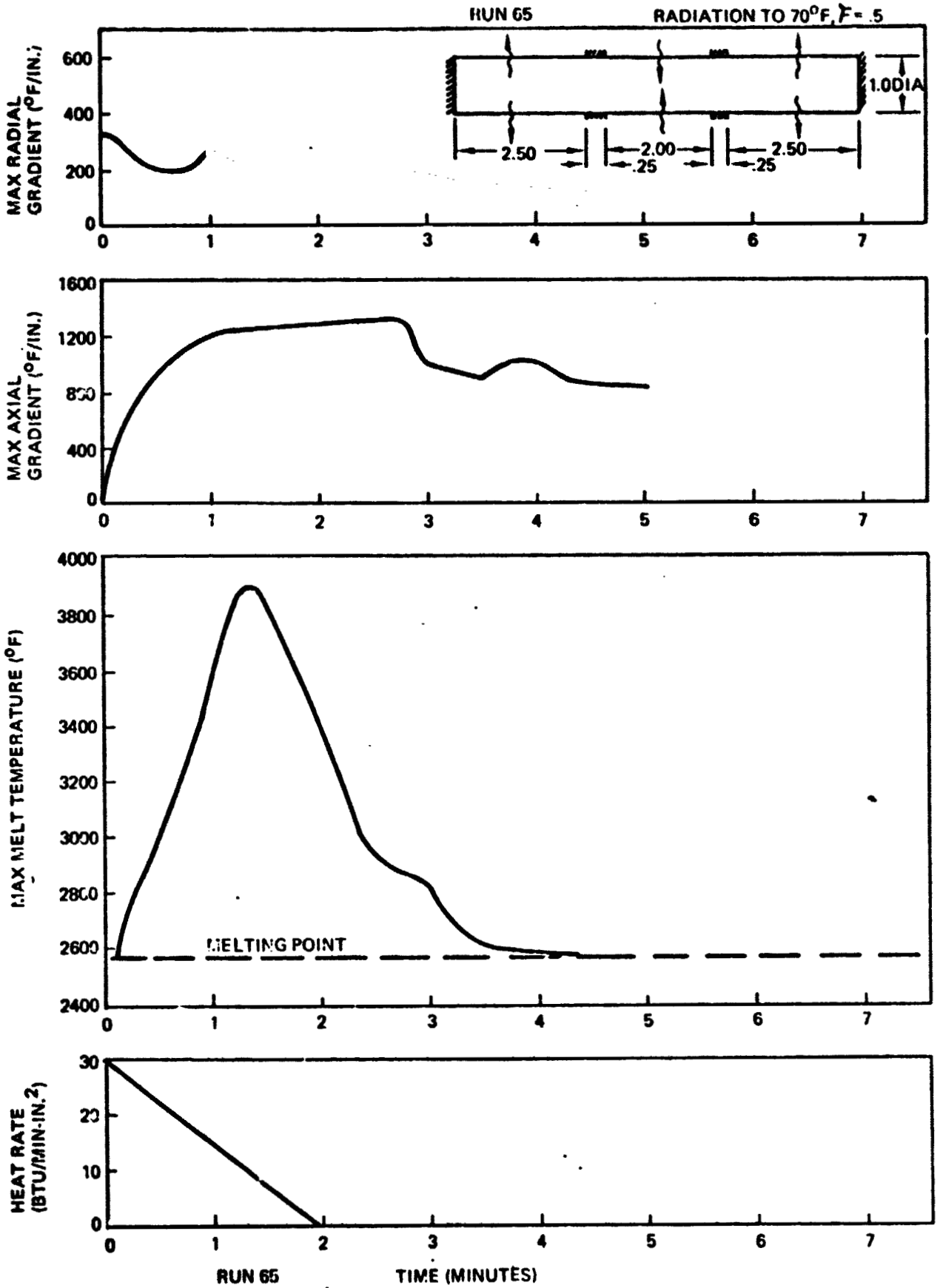

Figure 25

RUN 65 - TEMPERATURE GRADIENT & HEAT FLUX PROFILES

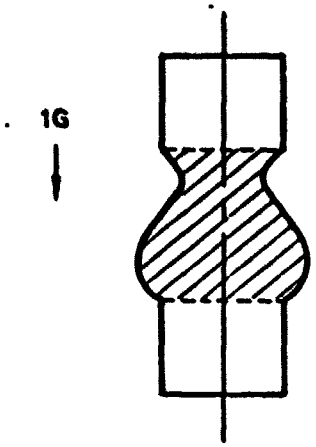

(a) VERTICAL CYLINDER WITH GRAVITY

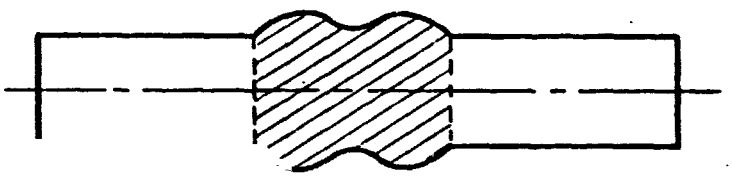

(b) FLOAT ZONE IN ZERO-G WITH ROTATION

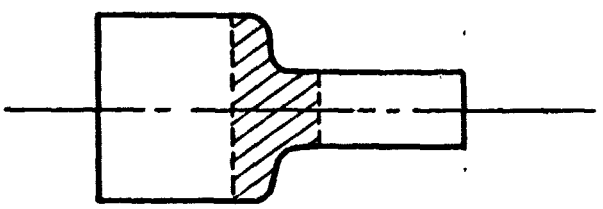

(c) FLOAT ZONE BETWEEN DIFFERENT DIAMETERS

FIGURE: 26 . *Typical Body-of-Revolution Configurations*

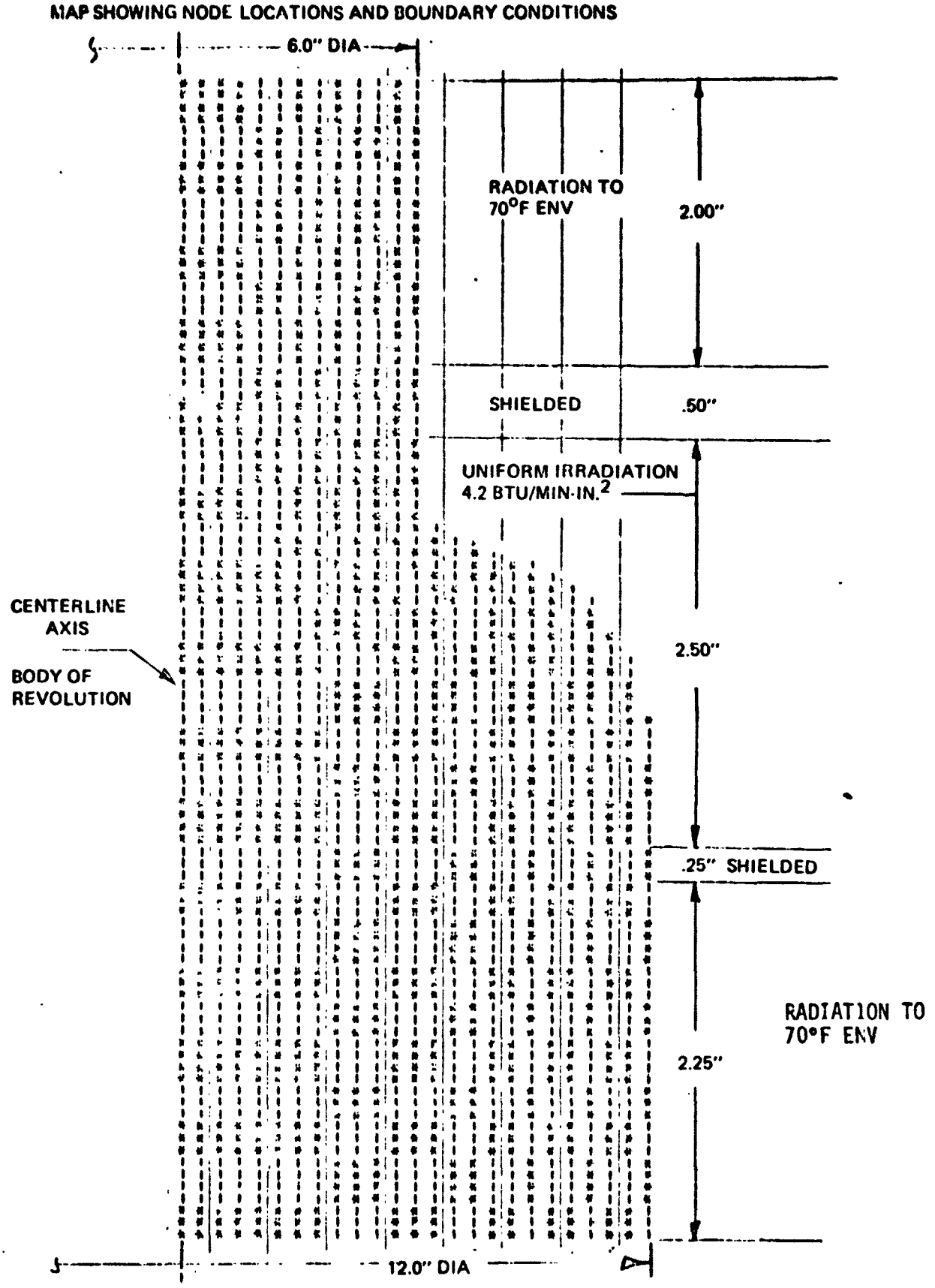

FIGURE: 27 *Run 80* BODY OF REVOLUTION NODE MAP

INITIAL CONDITIONS – TIME = 0
HEATING RATE = 551 BTU/MIN
COOLING RATE = 772 BTU/MIN

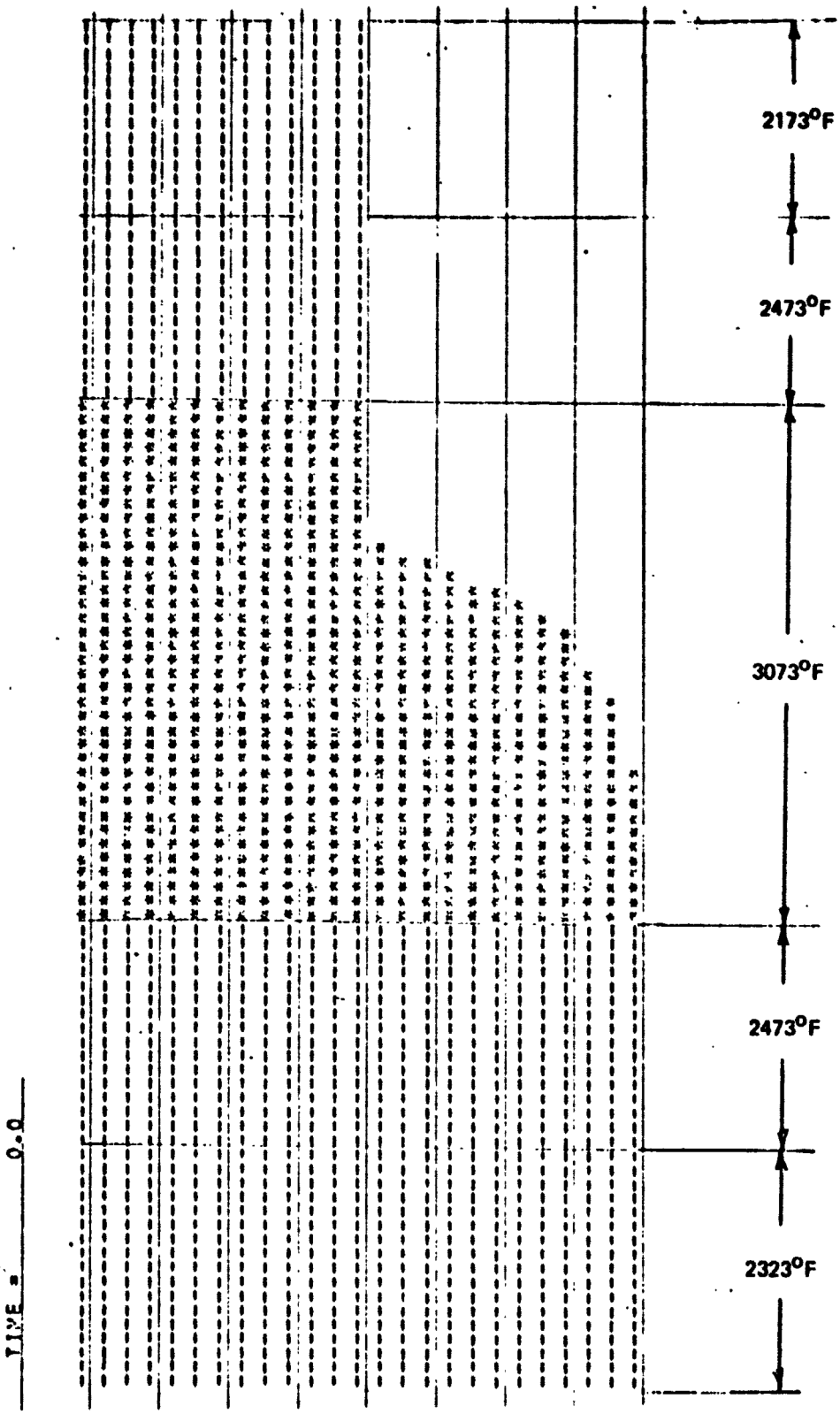

FIGURE: 28. *Run 80* - MELT ZONE - TIME = 0

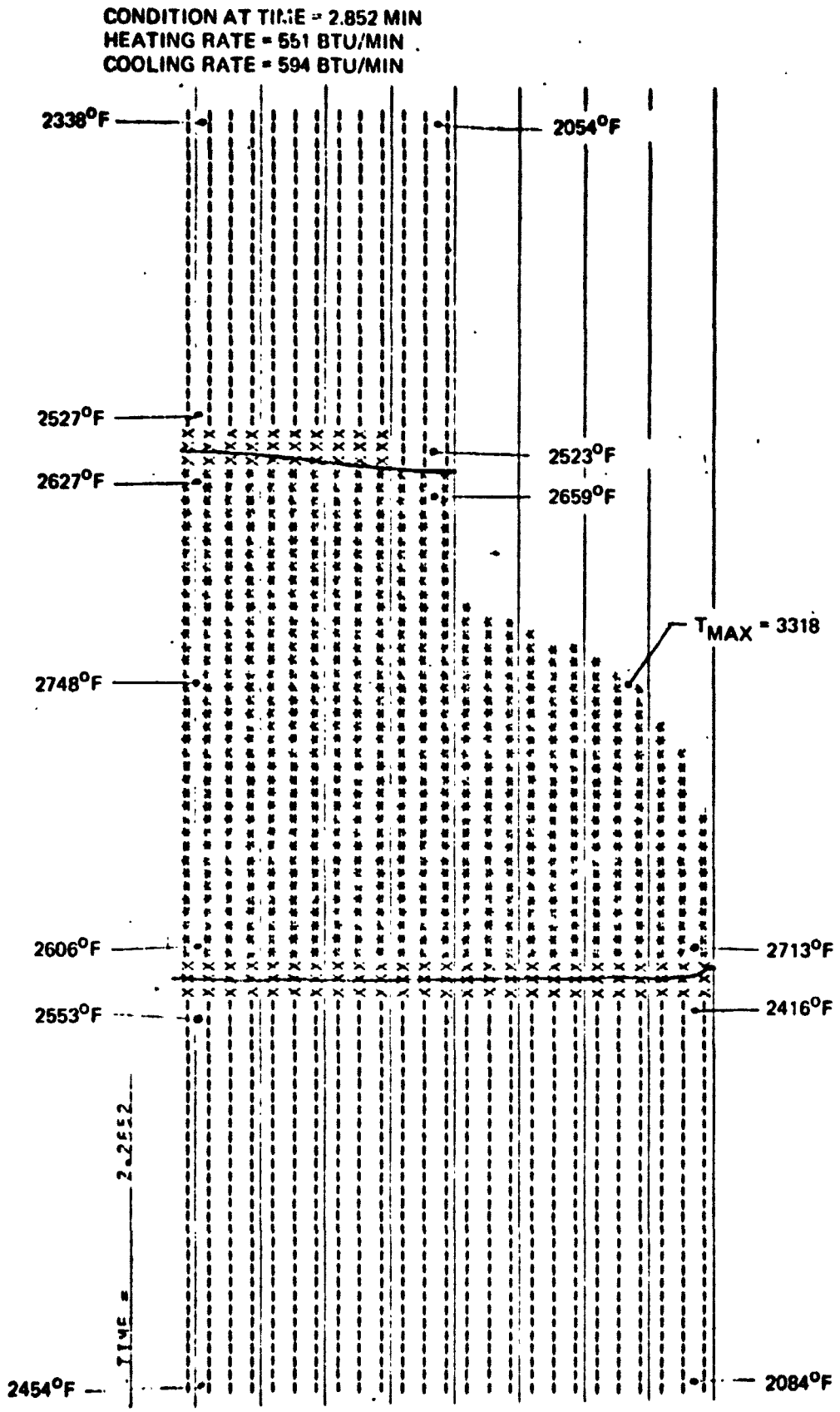

FIGURE: 29. *Run 80* - MELT ZONE - TIME = 2.852 MIN.

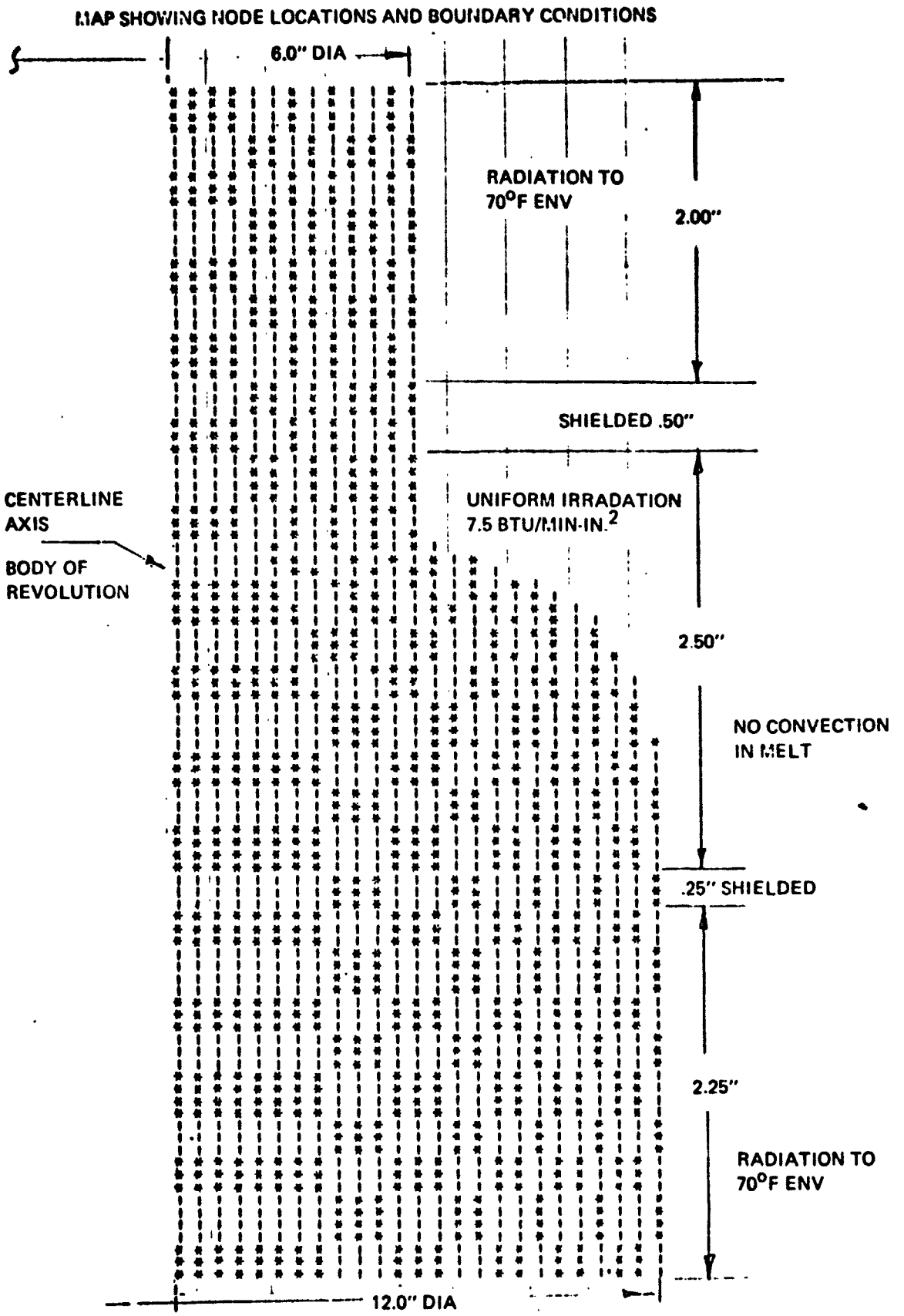

Figure 30. *Run 72* - MELT ZONE NODE MAP

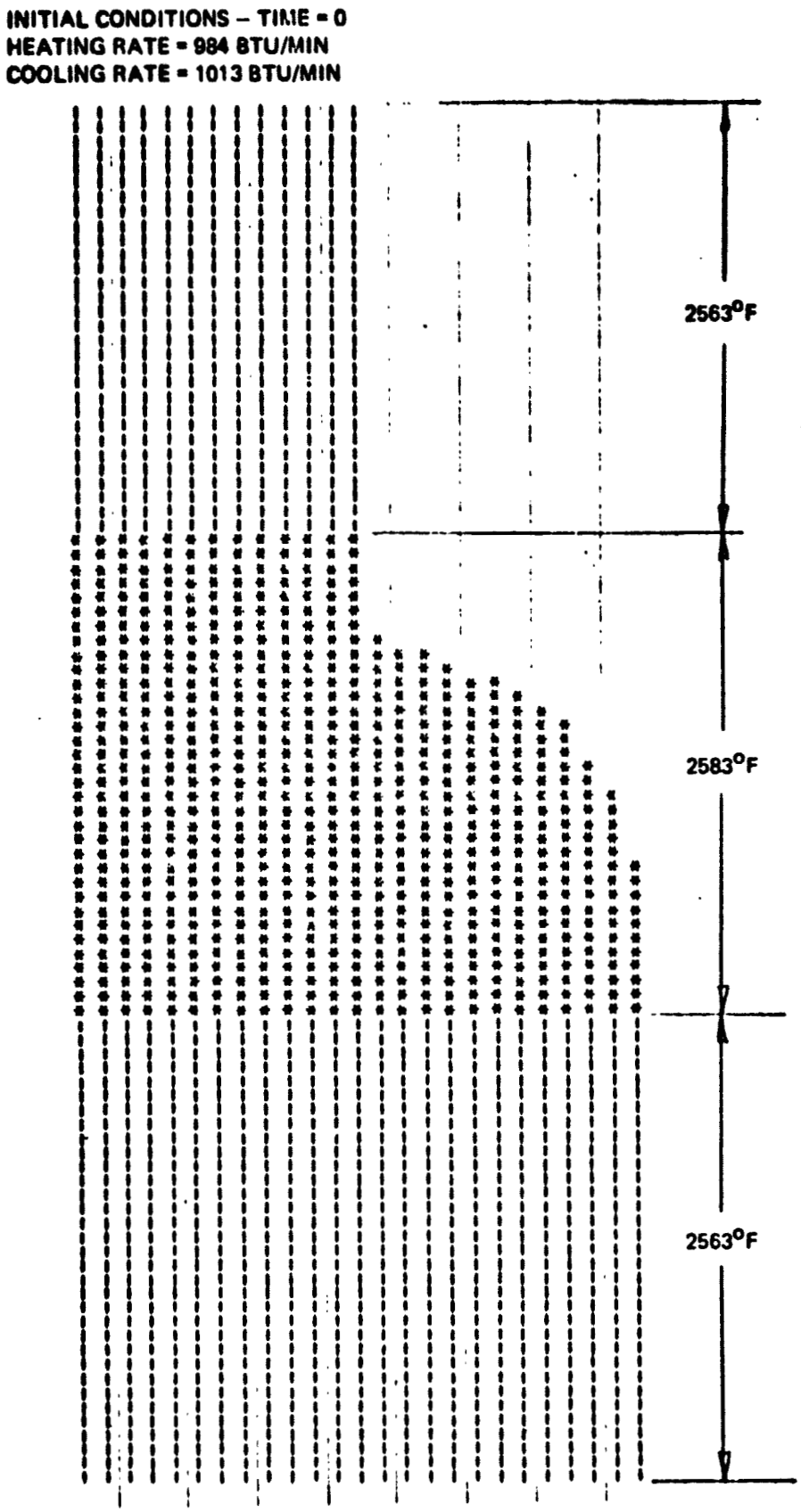

Figure 31. MELT ZONE TIME = 0 RUN 72

☆ U.S. GOVERNMENT PRINTING OFFICE 1976-641-255/420 REGION NO. 4

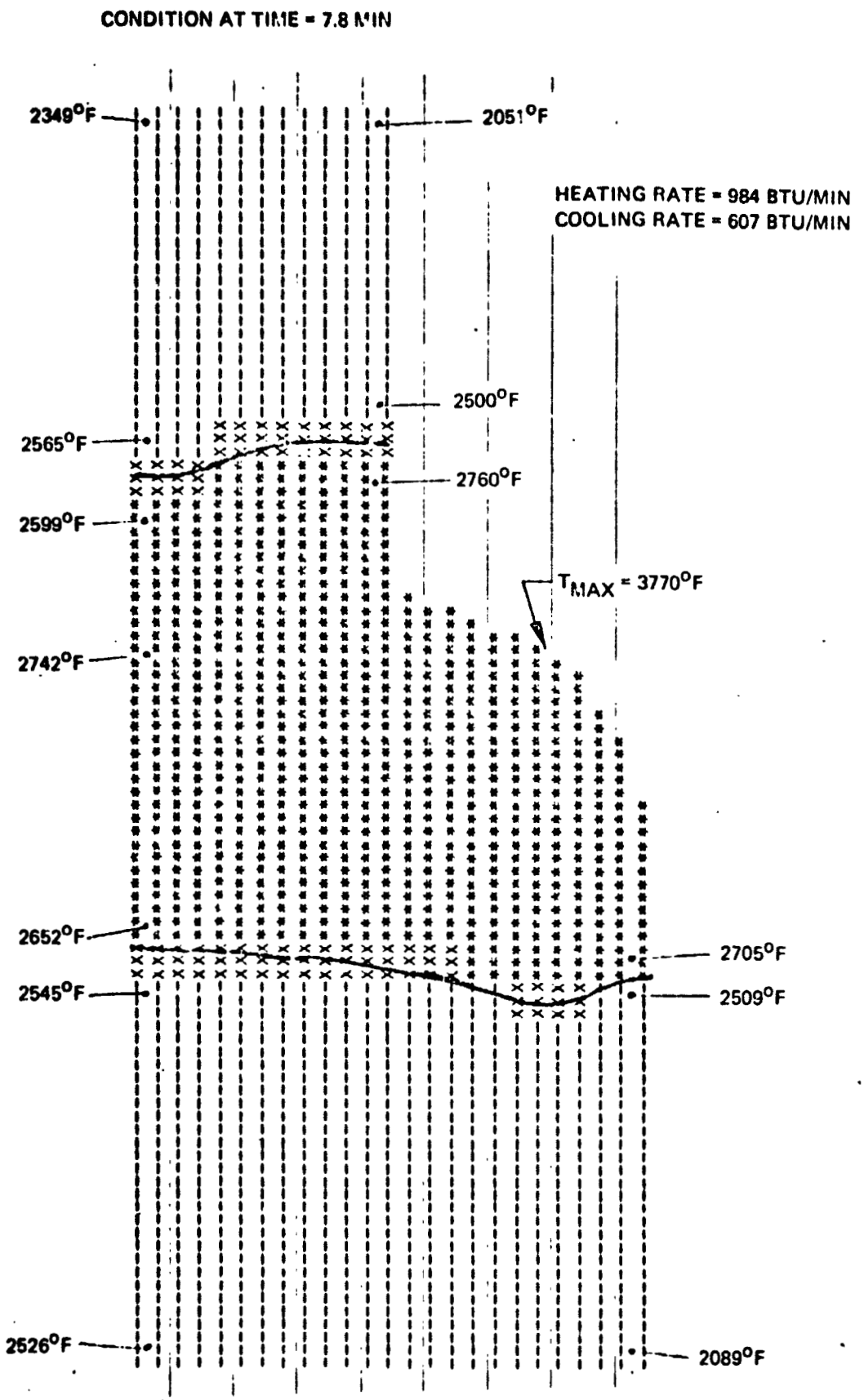

Figure 32. MELT ZONE TIME = 7.8 MIN. RUN 72